Int J Adv Struct Eng (2014) 6:69
DOI 10.1007/s40091-014-0069-y

ORIGINAL RESEARCH

Finite element code-based modeling of a multi-feature isolation system and passive alleviation of possible inner pounding

Mohammed Ismail · Francesc López-Almansa · Amadeo Benavent-Climent · Luis G. Pujades-Beneit

Received: 8 January 2014 / Accepted: 28 July 2014 / Published online: 15 August 2014

Abstract The existing seismic isolation systems are based on well-known and accepted physical principles, but they are still having some functional drawbacks. As an attempt of improvement, the Roll-N-Cage (RNC) isolator has been recently proposed. It is designed to achieve a balance in controlling isolator displacement demands and structural accelerations. It provides in a single unit all the necessary functions of vertical rigid support, horizontal flexibility with enhanced stability, resistance to low service loads and minor vibration, and hysteretic energy dissipation characteristics. It is characterized by two unique features that are a self-braking (buffer) and a self-recentering mechanism. This paper presents an advanced representation of the main and unique features of the RNC isolator using an available finite element code called SAP2000. The validity of the obtained SAP2000 model is then checked using experimental, numerical and analytical results. Then, the paper investigates the merits and demerits of activating the built-in buffer mechanism on both structural pounding mitigation and isolation efficiency. The paper addresses the problem of passive alleviation of possible inner pounding within the RNC isolator, which may arise due to the activation of its self-braking mechanism under sever excitations such as near-fault earthquakes. The results show that the obtained finite element code-based model can closely match and accurately predict the overall behavior of the RNC isolator with effectively small errors. Moreover, the inherent buffer mechanism of the RNC isolator could mitigate or even eliminate direct structure-to-structure pounding under severe excitation considering limited septation gaps between adjacent structures. In addition, the increase of inherent hysteretic damping of the RNC isolator can efficiently limit its peak displacement together with the severity of the possibly developed inner pounding and, therefore, alleviate or even eliminate the possibly arising negative effects of the buffer mechanism on the overall RNC-isolated structural responses.

Keywords Seismic isolation · Adjacent structures · Self-recentering · Buffer · Hysteresis · Pounding

M. Ismail (✉)
Structural Engineering Department, Zagazig University, Zagazig 44519, Egypt
e-mail: mohammed.ismail@upc.edu; mohammed.ismail_papers@yahoo.com

M. Ismail
Department of Applied Mathematics III, Technical University of Catalonia, 08034 Barcelona, Spain

F. López-Almansa
Architecture Structures Department, Technical University of Catalonia, 08028 Barcelona, Spain
e-mail: francesc.lopez-almansa@upc.edu

A. Benavent-Climent
Department of Structural Mechanics and Industrial Constructions, Technical University of Madrid, 28006 Madrid, Spain
e-mail: amadeo.benavent@upm.es

L. G. Pujades-Beneit
Department of Geotechnical Engineering and Geosciences, Technical University of Catalonia, 08034 Barcelona, Spain
e-mail: lluis.pujades@upc.es

Introduction

Structural engineers are challenged to design economic and visually appealing structures to safely withstand the forces of nature such as earthquakes, which significantly affect many areas of the world. Earthquakes generate forces as the building inertia resists motion while the foundation

shakes with the surrounding earth. Traditionally, building structures are designed to remain elastic during a weak earthquake. However, for a moderately strong or strong earthquake, the structures may behave inelastically resulting in cracks or residual deformations of the structures. Although the inelastic behavior of the main structural members provides structures with a source of energy dissipation, the resulting permanent deformations and cracks seriously affect the performance of structures and result in costly and difficult repair work.

Along time, many innovative methods have been developed, tested, and implemented for structural protection against earthquakes. Modern techniques for seismic hazard mitigation in structures include seismic isolation and energy dissipation systems. The principal function of an energy dissipation system is to reduce the inelastic energy dissipation demand on the framing system of a structure (Constantinou and Symans 1993). The result is reduced damage to the framing system. The added lateral stiffness may shift the periods of the relevant modes of vibration of the structure to a region of the response spectra where the seismic demands are higher. The added lateral strength may lead to higher component force demands, producing premature yielding, and high story accelerations, causing damage to contents. On the other hand, the concept of seismic isolation is to decouple the structure from the vibration source by means of a soft mechanical device, usually located between the structure and its foundation. Such an object filters the ground motion and shifts the natural period of the structure out of the range of dominant earthquake energy, increasing damping and limiting the force transfer. This strategy reduces the seismic forces to or near the elastic capacity of a structure, thus eliminating or reducing inelastic deformation and structural damage.

A successful seismic isolation system must incorporate seven basic elements. These are: (1) a rigid vertical mounting to support safely the structural weight, (2) a flexible horizontal mounting to lengthen the natural period of the structure, (3) a damping mechanism to control the relative deflections between the structure and the ground to a practical design level, (4) a means of providing adequate horizontal rigidity under low service load levels such as wind and minor earthquakes, (5) a recentering mechanism to re-center the isolated structure with the isolation system after earthquake as before earthquake, (6) a buffer or braking mechanism that imposes strict restrains on isolator motion after a certain chosen limit to avoid structural instability or destructive structural pounding under severe earthquakes, and (7) the isolation system must not have any critical inherent characteristic that may impair the isolated structure.

A variety of isolation devices including elastomeric bearings (with and without lead core), frictional, sliding and roller bearings have been developed, tested and implemented for aseismic design of structures during the last 30 years (Kelly 1986; Skinner et al. 1993; Naeim and Kelly 1999). In 1968, un-reinforced rubber blocks were first implemented into a reinforced concrete building in Macedonia but they bulged sideways under the weight the structure and led to building bounce and rocking (Staudacher 1982; Jurukovski and Rakicevic 1995). The subsequent development of laminated rubber bearings improved the vertical bearing capacity but without adding a source of damping. To combine flexibility and damping in a single unit, the lead rubber bearing (LRB) was invented in the 1970's (Robinson and Tucker 1977, 1983; Tyler and Robinson 1984). In the early 1980's, high damping rubber (HDR) bearings came into existence (Derham et al. 1985). However, both LRB and HDR isolation systems still lack a self-braking mechanism, under severe earthquakes, besides the aptitude for low-mass structures. In addition, they undergo bearing area reduction as displaced laterally, which imposes restrictions on the height/width and deformation/height ratios. In 1986, Al-Hussaini et al. (1994) introduced an isolation system, namely the friction pendulum system (FPS), which uses friction to dissipate the transmitted energy to the structure and concave sliding surfaces to provide a gravity-based recentering mechanism. Due to the concavity of sliding surfaces, a building supported on FPS isolators exhibits vertical fluctuation and vibrates as a simple pendulum having a constant vibration independent of the structural mass, which represents a severe practical difficulty that may lead to resonance failure as the FPS's period approaches the dominant period of the hitting earthquake (Murnal and Sinha 2004). Another drawback is the increase of sliding friction coefficient as sliding velocity increases as a characteristic of the interface liner of Teflon. Such increase of friction coefficient reduces the degree of structure–ground decoupling and results in more force transfer.

Recently, the Roll-N-Cage (RNC) isolator has been proposed (Ismail 2009; Ismail et al. 2008, 2009b, 2010) as an attempt of improvement, see Figs. 1 and 2. It is a rolling-based isolation system to achieve the maximum possible structure–ground decoupling and, therefore, minimizes the seismic force transfer. It is designed to achieve a balance in controlling isolator displacement demands and structural accelerations. It provides in a single unit all the necessary functions of vertical rigid support, horizontal flexibility with enhanced stability, hysteretic energy dissipation and resistance to minor vibration loads. Although the rolling core is quasi-ellipsoidal, the RNC isolator generates no vertical fluctuation of isolated structure during motion due to the inner curvatures of the upper and lower bearing plates. Moreover, the RNC isolator is distinguished by two unique features: (1) a self-braking

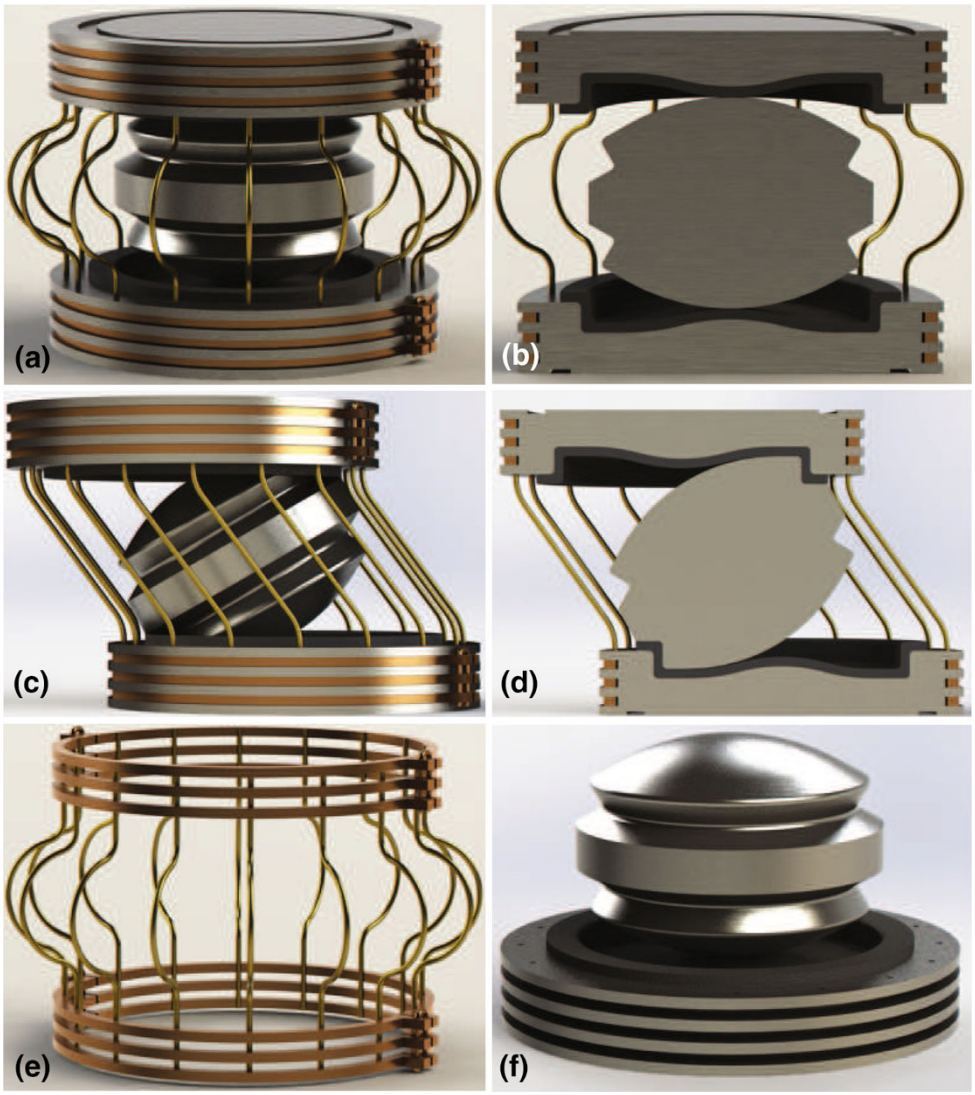

Fig. 1 The RNC isolator: **a** neutral position, **b** vertical cross-section at neutral position, **c** to-the-left maximum deformed position, **d** vertical cross-section at to-the-left maximum deformed position, **e** metallic yield dampers and their holders, **f** rolling core on the bottom rubber plate and the lower metallic bearing plate

(buffer) mechanism to limit the isolator displacement under severe seismic excitations to a preset value by the designer, as shown in Fig. 3 and (2) a linear gravity-based self-recentering mechanism that prevents residual displacement after earthquakes, as shown in Fig. 4. Such recentering mechanism is a result of adopting a quasi-ellipsoidal shape of the rolling core. Besides the rolling-based motion mechanism, which requires less lateral forces to initiate and maintain high degree of structure–ground decoupling compared to other motion mechanisms of the elastomeric-based and friction-based isolation systems, the RNC isolator is provided with a perfect design advantage to get the most benefit of that rolling-based motion mechanism. Such design advantage is the independency of both vertical bearing mechanism and the mechanism that provides lateral pre-yield stiffness against minor vibration loads. This independency allows for accurate tuning of the initial pre-yield stiffness to permit the commencement of the seismic isolation process, or decoupling, just after the seismic forces exceed the maximum limit of minor vibration loads, contrary to the available isolation systems. The RNC isolator can be available in different other forms to suit the structure or object to be protected, see Fig. 2a and b. More detailed description and thorough treatment of the RNC isolator are found in Ismail (2009) reference.

This paper attempts to provide a full-featured and handy modeling of a recently proposed multi-feature RNC isolator using a commercially available finite element-based code SAP2000 (SAP2000 documentation 2012). Such model aims at accurately incorporating all the main and unique features of the RNC isolator, away from mathematical complications, to provide a convenient and precise replacement of the RNC isolator in further professional studies and research works by both practicing structural designers as well as academic investigator. The resulting model is then validated using different, previously

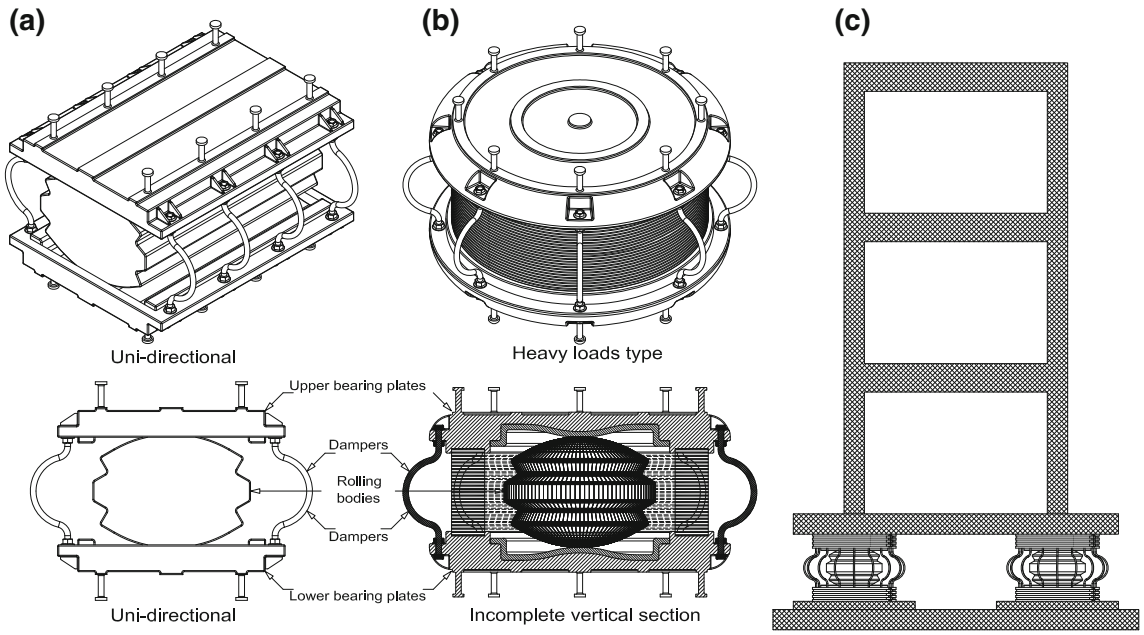

Fig. 2 **a** A design of the RNC isolator for unidirectional isolation of light- to moderate-mass structures, **b** a design of the RNC isolator for multidirectional isolation of heavy-mass structures, **c** the RNC-isolated structural model

obtained, force–displacement representations of the RNC isolator. Then, the obtained SAP2000 model is numerically implemented into a case study to investigate the influence of activating its buffer mechanism on the structural response considering severe uni and bidirectional near-fault ground motions. Finally, the paper attempts to passively alleviate the possibly arising negative effects due to the buffer activation of the RNC isolator.

The force–displacement relationship of the RNC isolator

The mechanical characterization of an innovative system or a device is often performed both experimentally and via numerical simulation. The former approach, which is more costly than the later one, leads directly to the physical understanding of the system and, therefore, it can be employed for final verification. In contrast, numerical simulation which uses numerical methods such as finite element method (FE) to quantitatively represent the evolution of a physical system and allows for more economically exploring a large number of possible design solutions. Using accurate models, the result of such simulations can give a good representation of the real mechanical behavior of the studied device or of the complex system which comprises the device. This accuracy enables safe drawing of proper conclusions and getting a thorough understanding of the system.

The RNC isolator has been subjected to thorough numerical characterization in Ismail et al. (2009b, 2010), experimental verification in Ismail and Rodellar (2014a, b) and full mathematical modeling in Ismail et al. (2013). The resulting unique force–displacement relationship of the RNC isolator is demonstrated schematically in Fig. 5. Based on Fig. 5, the mathematical description of the total RNC isolator's restoring force, F_b, is obtained by superimposing the following three individual restoring components:

1. Self-recentering component, F_{bR}
2. Hysteretic component, F_{bH}
3. Self-braking (buffer) component, F_{bB}.

According to Ismail et al. (2013), the total restoring force of the RNC isolator is expressed mathematically according to the relationship between the actual displacement of the RNC isolator and its preselected design displacement x_{des} as:

$$F_b = \begin{cases} F_{bH} + F_{bR} & \text{if } |x_b| < x_{des} \\ F_{bH} + F_{bR} + F_{bB} & \text{if } |x_b| > x_{des} \end{cases} \quad (1)$$

Based on Fig. 5, the main controlling parameters of the RNC isolator's hysteresis loop shape are:

- Yield displacement D_y,
- Yield strength F_y of the hysteretic metallic yield dampers,
- Maximum restoring forces $(F_{bH} + F_{bR})$ and $(F_{bH} + F_{bR} + F_{bB})$

- Maximum displacement D_{max},
- Elastic (pre-yield) stiffness k_e defined as: $\frac{F_y}{D_y}$,
- Plastic (post-yield) stiffness k_p,
- Buffer stiffness k_B,
- Effective stiffness k_{eff} defined as: $\frac{(F_{bH}+F_{bR})}{x_{des}}$,
- Total effective stiffness k_{eff-T} defined as: $\frac{(F_{bH}+F_{bR}+F_{bB})}{D_{max}}$,
- characteristic strength Q,
- The yielding exponent n, which controls the curvature at the hysteresis loop corners.

Based on Figs. 3 and 5, the behavior of the RNC isolator just after exceeding the design displacement x_{des} could be explained. The integrated buffer has a unique stiffness k_B, which is always higher than the dampers stiffness. The k_B is activated only after exceeding the design displacement and it is represented with the steeper slope in Fig. 5 in the first and the third quadrants. The activation of the buffer stiffness means deactivation of the dampers stiffness and conversely. The less steep slope is attributed to the less stiff metallic yield dampers, which are reactivated again when the buffer mechanism becomes deactivated as the RNC isolator reaches the end of stroke and start to reverse its direction of motion.

Similarly, it is worth explaining why the gravity-based recentering mechanism of the RNC isolator is unique and it is not traditional. The integrated passive recentering mechanism of the RNC isolator can provide gravity-based recentering force without generating any undesired side

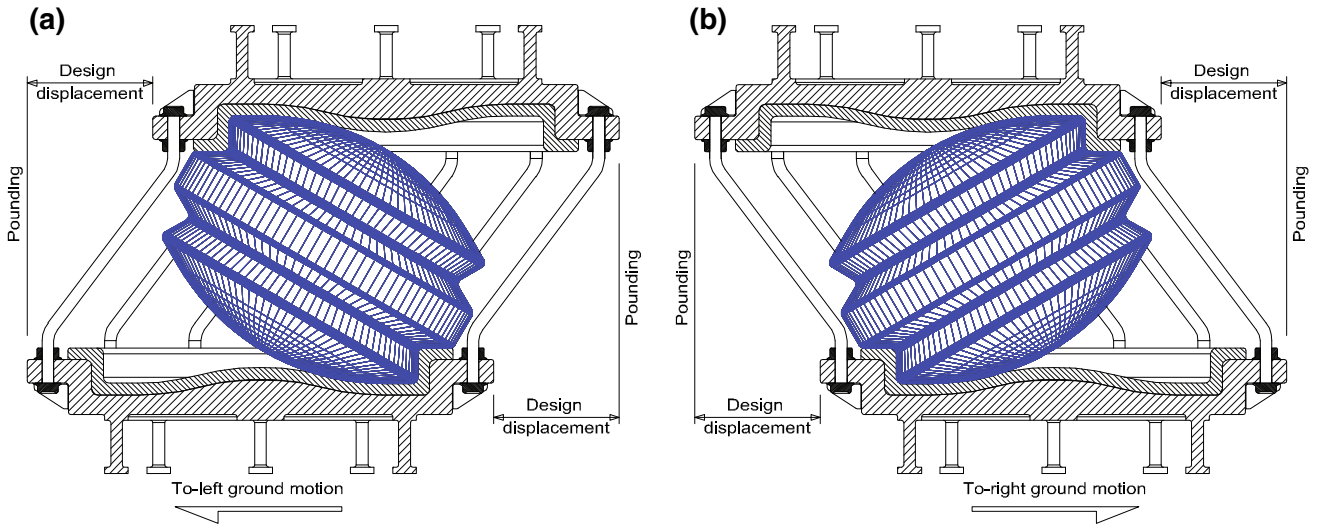

Fig. 3 The RNC isolator buffer mechanism after a certain design displacement: **a** vertical cross-section at maximum to-the-right deformed position, **b** vertical cross-section at maximum to-the-left deformed position

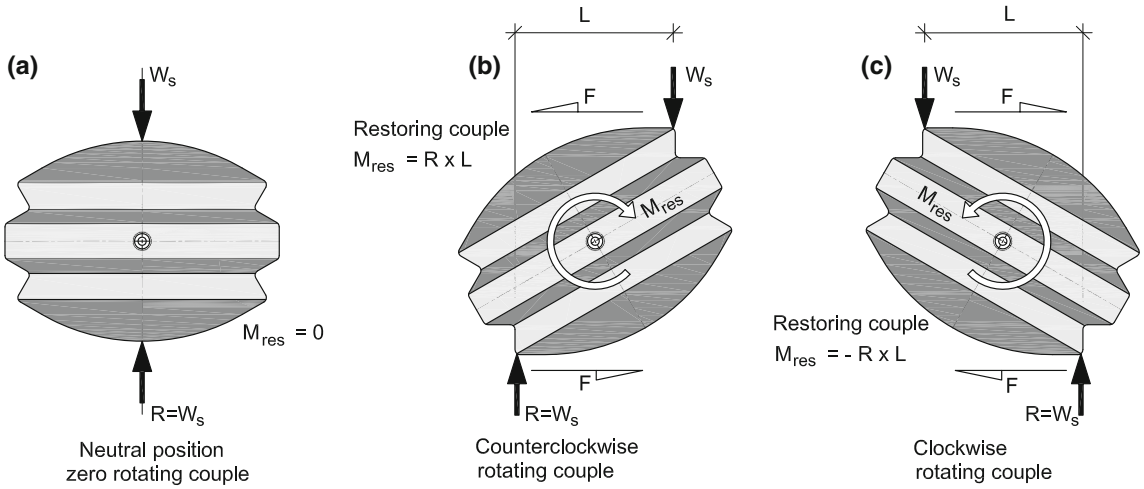

Fig. 4 The integrated recentering mechanism of the RNC isolator: **a** neutral position, **b** to-the-left deformed position, **c** to-the-right deformed position

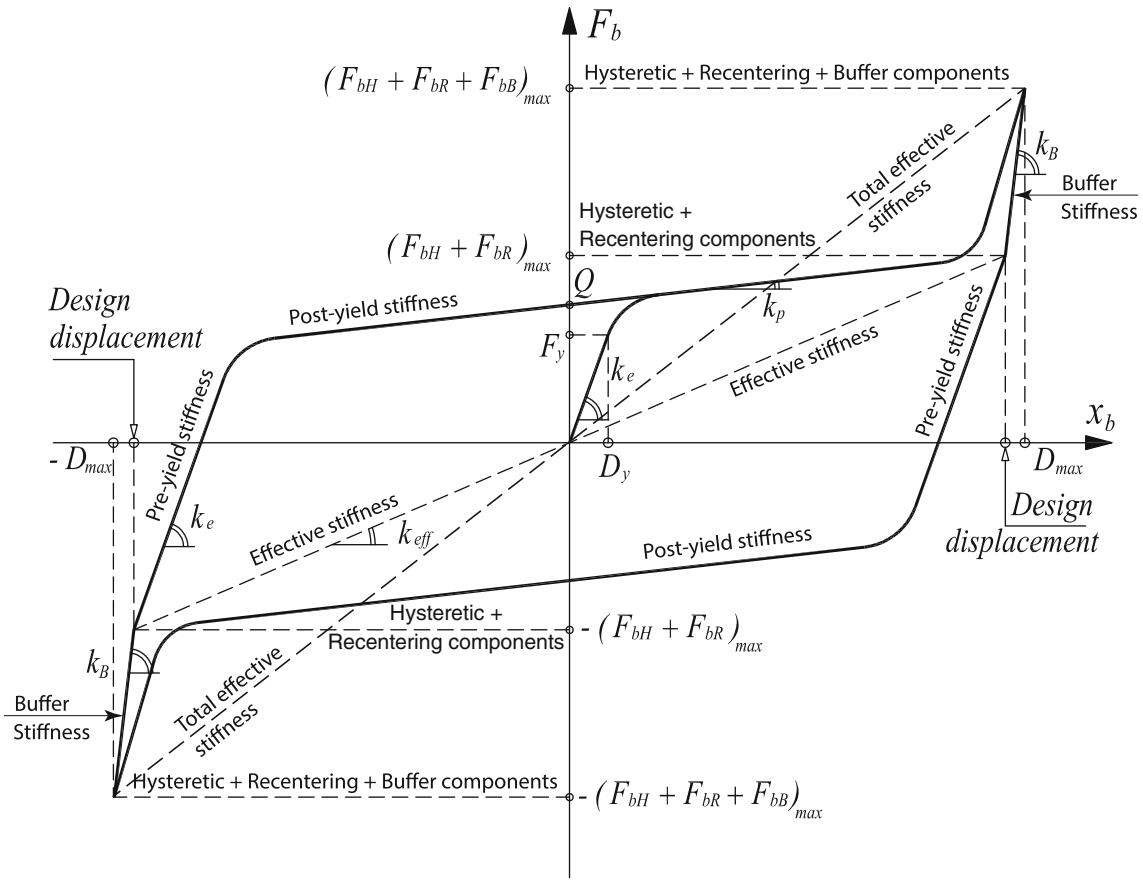

Fig. 5 Force–displacement relationship of RNC isolator

effects. Several available traditional isolation devices [such as springs, elliptical and friction pendulum systems (FPS)] can provide some recentering forces but they are always accompanied by the generation of vertical accelerations out from the horizontal acceleration components, which leads to additional vertical vibration of structural elements, housed inner equipment and occupants discomfort. Moreover, the configurations that provide such recentering forces in elliptical and FPS isolation systems force the isolated structure to oscillate as a simple pendulum with a single vibration period, which may be close to the dominant period of the exciting earthquake causing resonance unlike the RNC isolator. In the RNC isolator, although the rolling core is ellipsoidal to provide adequate eccentricity for gravity-based recentering, the upper and lower bearing plates are provided with carefully designed inner curvatures (facing the rolling core) to exactly absorb any generated vertical displacement that arises from rolling of the elliptical core. This always keeps the vertical offset between the upper and the lower bearing plates unchanged during the RNC isolator motion, which theoretically prevents the generation of vertical motion component out from the horizontal one, leading to a unique recentering behavior of the RNC isolator.

Factor of safety against sliding motion of the rolling core

The RNC isolator is configured to force only the rolling motion of its rolling core. The relative sliding motion was not allowed during the performed numerical and experimental characterization of the device or during deriving a full mathematical representation of its main and unique features. Any slip between the rolling core and the upper and lower plates is avoided, based on the following:

- The existence of two Neoprene or rubber plates between the rolling core and both upper and lower bearing steel plates. These rubber plates are completely adhered to the upper and lower bearing steel plates, but they are in direct rolling contact with the upper and lower spherical surfaces of the rolling core. One of their main roles is to improve the friction coefficient with the rolling core surfaces to force only rolling motion and prevent sliding.
- The upper and lower spherical surfaces of the rolling core have small regular roughness to better increase the friction coefficient with the upper and lower rubber plates (Ismail 2009).

– The inner curvatures of the upper and lower bearing plates (facing rolling core) were designed to prevent vertical uplift while keeping adequate safety against sliding (Ismail 2009).

To determine the factor of safety (FOS) against sliding of the rolling core inside the RNC isolator at an instant of time, let's refer to Fig. 6 and consider only the developed internal forces inside that core at a certain inclination angle α, between the neutral and the farthest deformed positions. Considering the upper contact point A between the rolling core's top surface and the upper bearing plate's lower surface, an upward reaction R_1 is developed due to the downward structural weight W_s. The reaction R_1 is decomposed into two components, normal and parallel-to-tangent at point A, referred to as F_{n1} and F_{p1}, respectively. According to the design principles of the RNC isolator (Ismail 2009), the steepest tangent slope of the inner triple curvatures of the upper and lower bearing plates α_{max} is 15°. Assume a static coefficient of friction between the contact surfaces μ. The parallel-to-tangent friction force μF_{n1} stabilizes the rolling core against sliding, while the parallel-to-tangent component F_{p1} is the destabilizing one which compels sliding. Therefore, the FOS against sliding is expressed as:

$$\mathrm{FOS}_{\mathrm{sliding}} = \frac{\mu F_{n1}}{F_{p1}} = \frac{\mu R_1 \cos(\alpha_{max})}{R_1 \sin(\alpha_{max})} = 3.73\mu \qquad (2)$$

The static coefficient of friction μ is 0.74 for steel on steel and 0.90 for steel on rubber (Grigoriev et al. 1996). Therefore, the $\mathrm{FOS}_{\mathrm{sliding}}$ ranges from 2.76 to 3.36. Similarly, the $\mathrm{FOS}_{\mathrm{sliding}}$ when considering the lower point of contact B is high enough to avoid sliding motion of the rolling core of the RNC isolator.

SAP2000 modeling of the RNC isolator

The objective of this Section is to develop a full-featured and handy model of the recently proposed RNC isolator using SAP2000 (SAP2000 documentation 2012), an available sophisticated FE software in the area of structural engineering. SAP2000 is an integrated stand-alone finite element-based structural program, introduced over 30 years ago, for the analysis and design of civil structures. SAP2000 is object-based, meaning that the models are created using members that represent the physical reality. Then, it automatically converts the object-based model into an element-based model that is used for analysis. This element-based model consists of traditional finite elements and joints (nodes). Results of the analysis are reported back on the object-based model. In this paper, the term "element" will be used more often than "object", since it is directly related to the FE analysis.

In this section, each of the three previously modeled features of the RNC isolator (recentering, damping and buffer) are modeled separately using one of the available properties of the Link/Support built-in element of SAP2000. Then, combined together to constitute a comprehensive model that matches the derived mathematical model in Eq. (1) and the force–displacement relationship shown in Fig. 5. "Modeling of the RNC isolator's hysteretic damping mechanism in SAP2000" section models the RNC isolator's hysteretic damping mechanism first, as it represents the fundamental behavior of the RNC isolator. Then, the other two unique features of self-recentering and self-braking mechanisms are modeled in "Modeling of the RNC isolator's self-recentering mechanism in SAP2000" and "Modeling of the RNC isolator's self-braking (buffer) mechanism in SAP2000", respectively.

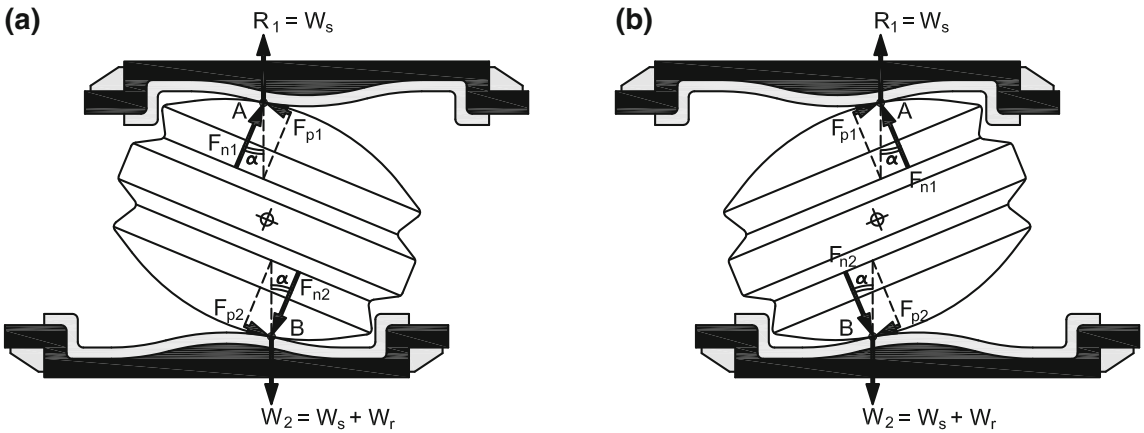

Fig. 6 Safety against sliding of the rolling core: **a** to-the-right rotation, **b** to-the-left rotation

Modeling of the RNC isolator's hysteretic damping mechanism in SAP2000

Although the above form of the Bouc–Wen model, which is used to model the hysteretic behavior of the RNC isolator, has been extensively used to describe nonlinear hysteretic behaviors in seismic isolation systems, it was proved that the parameters of that Bouc–Wen model form are functionally redundant; that is, there exist multiple parameter vectors that produce an identical response from a given excitation by Constantinou and Adnane (1987) and Ma et al. (2004). Constantinou and Adnane (1987) suggested imposing the constraint $\frac{A}{\beta+\gamma} = 1$ to reduce the model to a formulation with well-defined properties. Ma et al. (2004) recommended that removing this redundancy is best achieved by setting $A = 1$.

The hysteretic behavior of the RNC isolator can be modeled using the Wen plasticity property in SAP2000. Such plasticity model is based on the hysteretic behavior proposed by Wen (1976), see Fig. 7 after eliminating the redundant parameters (SAP2000 documentation 2012). An independent uniaxial Wen plasticity property can be assigned to any deformational degree of freedom, keeping all the internal deformations independent. The hysteretic behavior of the RNC isolator F_{bH} can be represented by the nonlinear force–deformation relationship of the Wen plasticity property in SAP2000 as:

$$F_{\mathrm{bH}} = \mathrm{ratio}\ k\ d + (1 + \mathrm{ratio})\ \mathrm{yield}\ z \tag{3}$$

where k is the elastic spring constant, yield is the yield force, ratio is the specified ratio of post-yield stiffness to elastic stiffness k, and z is an internal hysteretic variable. This variable has a range of $|z| \leq 1$, with the yield surface represented by $|z| = 1$. The initial value of z is zero, and it evolves according to the differential equation:

$$\dot{z} = \frac{k}{\mathrm{yield}} \begin{cases} \dot{d}(1 - |z|^{\mathrm{exp}}) & \text{if } \dot{d}\, z > 0 \\ \dot{d} & \text{otherwise} \end{cases} \tag{4}$$

where exp is an exponent greater than or equal to unity. Larger values of this exponent increases the sharpness of yielding in the hysteresis loop. The practical limit for exp is about 20.

It is worth stressing that the Wen plasticity property in SAP2000 is based on the work of Constantinou and Adnane (1987) and Ma et al. (2004). This means that the Eq. (4) is equivalent to the standard Bouc–Wn model after setting $A = 1$ and $\beta = \gamma = 0.50$ to eliminate redundancy of the original model parameters (SAP2000 documentation 2012).

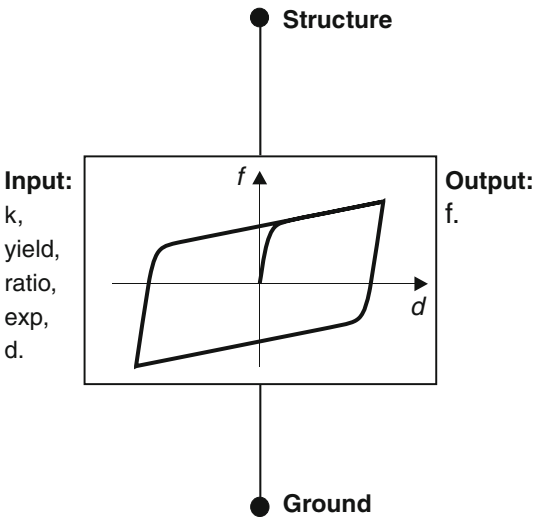

Fig. 7 Wen plasticity property type for uniaxial deformation used in SAP2000

Modeling of the RNC isolator's self-recentering mechanism in SAP2000

The linear self-recentering force of the RNC isolator can be represented simply by a horizontal linear spring property in SAP2000, see Fig. 8a. A force equivalent to the linear recentering force F_{bR} of the RNC isolator can be represented by the simple force–deformation relationship for a uniaxial linear spring property as:

$$F_{\mathrm{bR}} = k\ d \tag{5}$$

where k is the spring constant and d is the deformation across the spring.

Modeling of the RNC isolator's self-braking (buffer) mechanism in SAP2000

The self-braking (buffer) feature of the RNC isolator can be modeled in SAP2000 using two Link/Support properties: the Gap or "compression-only" property and the Hook or "Tension-only" property. Both properties can be assigned to any deformational degree of freedom independently. The opening or closing of a gap for one deformation does not affect the behavior of the other deformations. Using the Gap property, Fig. 8b, the restoring buffer component of the RNC isolator can be represented by the following nonlinear force–deformation relationship:

$$F_{\mathrm{bB}} = \begin{cases} k\ (d + \mathrm{open}) & \text{if } (d + \mathrm{open}) < 0 \\ 0 & \text{otherwise} \end{cases} \tag{6}$$

where k is the spring constant, and open is the initial gap opening, which must be zero or positive. Using the Hook

property, Fig. 8c, the restoring buffer component of the RNC isolator can be represented by the following nonlinear force–deformation relationship:

$$F_{\mathrm{bB}} = \begin{cases} k\ (d - \mathrm{open}) & \text{if } \ (d - \mathrm{open}) > 0 \\ 0 & \text{otherwise} \end{cases} \tag{7}$$

where k is the spring constant, and open is the initial hook opening, which must be zero or positive. According to Eqs. (6) and (7), the behavior of both Gap and Hook properties is identical except the force sign, as the Gap property always supports compressive forces while the Hook property supports only tensile forces. Since the buffer mechanism of the RNC isolator restrains motion through compression, Fig. 3, the concept of the Gap property matches better than that of the buffer mechanism of the RNC isolator.

Finally, the overall FE representation of the RNC isolator using the built-in SAP2000 elements is shown in Fig. 9b. Such SAP2000 representation of the RNC isolator takes into account the following inherent characteristics of the device:

- Self-recentering,
- Hysteretic damping,
- Self-braking,
- Design displacement,
- Vertical rigidity,
- Horizontal flexibility,
- No uplift,
- Pre-yield stiffness.

Verification of the obtained full mathematical and SAP2000 models for the RNC isolator

The obtained full-feature SAP2000 model of the RNC isolator is subjected to deep numerical, analytical and experimental validation in this section. Both numerical and analytical verification are presented in "Numerical and analytical verification", while the experimental validation is presented in "Experimental validation". The discrepancy between the measured and predicted outputs, F_{m} and F_{bH}, is then quantified using the L_1 and L_∞-norms and the corresponding relative errors ε:

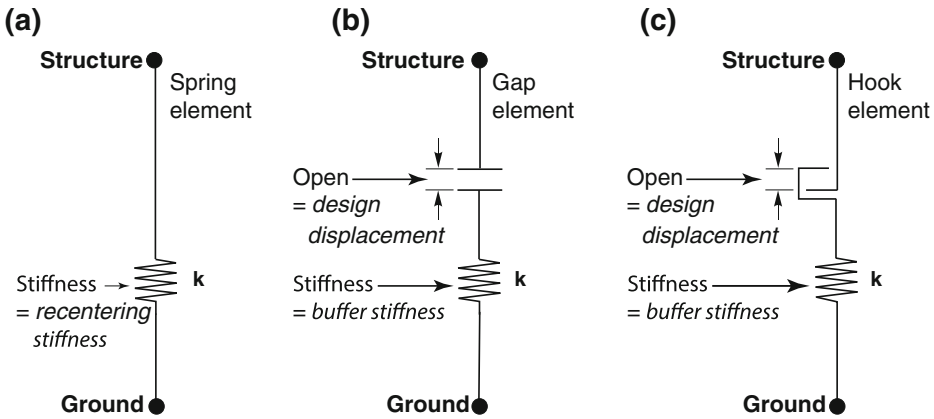

Fig. 8 **a** Spring property, **b** gap property, **c** Hook property types for uniaxial deformations used in SAP2000

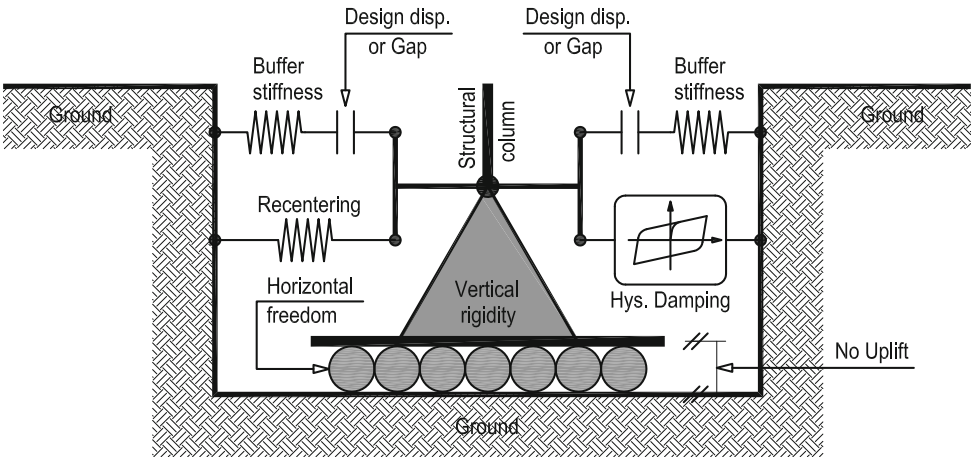

Fig. 9 Full modeling of the RNC isolator using SAP2000's elements

$$||f||_1 = \int_0^{T_e} |f(t)|\mathrm{d}t \tag{8}$$

$$||f||_\infty = \max_{t\in[0,T_e]} |f(t)| \tag{9}$$

$$\varepsilon_{1,\infty} = \frac{||F_m - F_b||_{1,\infty}}{||F_m||_{1,\infty}} \tag{10}$$

The relative error ε_1 quantifies the ratio of the bounded area between the output curves to the area of the measured force along the excitation duration T_e, while ε_∞ measures the relative deviation of the peak force.

Numerical and analytical verification

In this section, the validity of the obtained complete mathematical model, expressed by Eq. (1), and the full SAP2000 model, illustrated in Fig. 9b, of the RNC isolator are checked in five steps:

1. Design an example of the RNC isolator, as shown in Fig. 10, following the design methodology found in Ismail (2009). The designed example allows for a design displacement of 300 mm, after which is directly activated.
2. Finite element mechanical characterization of the designed isolator example, as shown in Figs. 11 and 12 and as explained in Ismail et al. (2009b), to obtain the "measured" force–displacement relationship (similar to what is explained in "The force-displacement relationship of the RNC isolator").
3. Mathematical modeling of the designed isolator example using Eq. (1) to obtain the mathematically predicted force–displacement relationship, as explained in "The force-displacement relationship of the RNC isolator" and Ismail et al. (2013).
4. SAP2000 modeling of the designed isolator using the developed model illustrated in Fig. 9b to obtain the SAP2000 force–displacement relationship, as explained in "SAP2000 modeling of the RNC isolator". The SAP2000's model parameters of the designed example are listed in Table 1. Their values are based on the geometry of the finite element force–displacement relationship in Step 2 and are obtained following the methodologies in Ikhouane and Rodellar (2005), Ikhouane et al. (2007) and Ismail et al. (2009a).
5. Comparing the "mathematical" (obtained in step 3) and "SAP2000" (obtained in step 4) force–displacement relationship with the "measured" one (obtained in step 2) and then examining the relative errors using Eqs. (8), (9) and (10), see Table 2.

Figures 13, 14 and 15 show the total restoring forces of RNC isolator under El-Centro, Kobe and Northridge earthquakes, respectively, in time scale. In each figure, three total restoring forces are plotted together for the purpose of clear comparison: (1) the "measured" total restoring force obtained from the FE characterization of the RNC isolator example as in Step 2, (2) the "mathematical" total restoring force predicted by the developed mathematical model as in Step 3, and (3) the "SAP2000" total restoring force calculated using the developed SAP2000 model as in Step 4. The relative errors, ε_1 and ε_∞, are listed in Table 3 for all cases shown in Figs. 13, 14 and 15. Based on the close matching of the three total restoring forces shown in Figs. 13, 14 and 15 together with the relatively small relative error percentages in Table 3, a main conclusion can be drawn. Such main conclusion is: both of the developed complete mathematical model, Eq. (1), of the RNC isolator and its full implementation using the SPA2000 built-in elements, Fig. 9b, are powerful representatives for the RNC isolator and, therefore, they could be considered as effective substitutions of the RNC isolator for more future studies.

Experimental validation

A set of 1/10 reduced-scale prototype of the RNC isolator has been designed based on the maximum allowed horizontal displacement to be used in the experimental mechanical characterization of the RNC isolator, in addition to the subsequent experimental assessment of its efficiency through implementation into a small-scale building model and equipment isolation in the near future. Figure 10 shows the dimensions in millimeters of the real-scale design of the RNC isolator, which has been reduced to a 1/10 scale to carry out the required experimental validation of the RNC isolator. Figure 16a shows a constructed sample of the used 1/10 reduced-scale experimental prototypes, which is made of stiff-aluminum, with a vertical load design capacity of around 4,000.0 N. Figure 16b shows the experimental prototype during dynamic testing. More information on the experimental characterization of the RNC isolator is found in Ismail and Rodellar (2014a, b). It is worthwhile to mention that all experimental tests were directly supported and entirely funded through the director of the CoDAlab research group and are carried out using the whole facilities of the CoDAlab laboratory in Spain.

The experimental force–displacement relationship of the RNC isolator prototypes is shown in Fig. 17a and b against

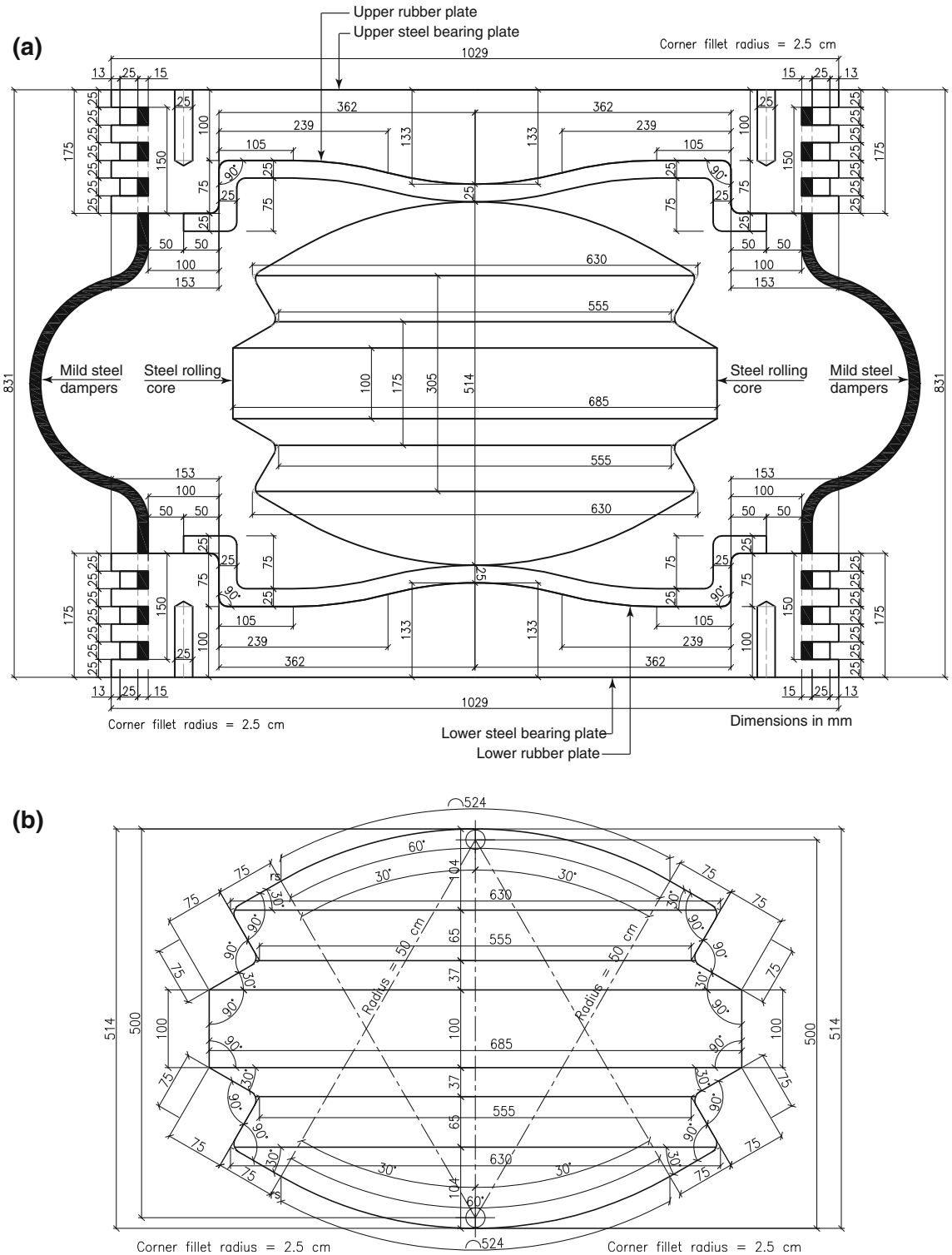

Fig. 10 Full dimensions of a designed RNC isolator, having a design displacement of 300 mm, used in this study: **a** sectional front view of the full isolator, **b** front view of the rolling core

analytical (Ismail et al. 2013), and SAP2000 outputs as a result of reduced-amplitude synthetic sinusoidal and real Kobe earthquakes. Both analytical and SAP2000 outputs are tuned using trail and error method to closely match the experimental output. As a result, the discrepancy is manually minimized between the three different force–

displacement relationships under each of the two considered excitations. Table 3 lists the relative errors, ε_1 and ε_∞, between the total restoring forces of the RNC isolator under the two reduced-amplitude earthquakes considering three outputs; the experimentally measured, the mathematical, and the SAP2000 total restoring forces. Effectively, the errors are small enough to lead nearly to the same results considering any of the three RNC isolator models. Although the errors of both experimentally measured and mathematical approaches are smaller, the use of these two models is much more complicated and time consuming than using the handy SAP2000 model. In other words, regarding flexibility, versatility, computation efforts, ease of use and wide sets of users, the SAP2000 model could represent another more practical alternative to express the RNC isolator behavior without sacrificing or losing the modeling accuracy. Therefore, one main conclusion could be drawn, which is the developed model of the RNC isolator using SPA2000 is a powerful representative for the device in this study and further future professional or academic research studies.

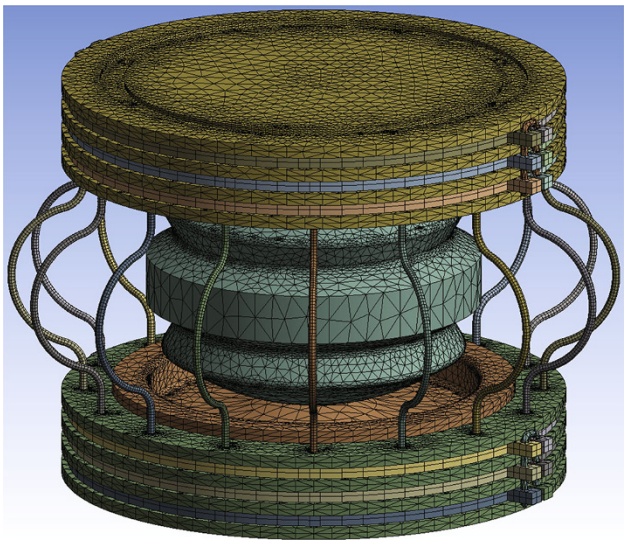

Fig. 11 Finite element meshing of the RNC isolator, neutral position

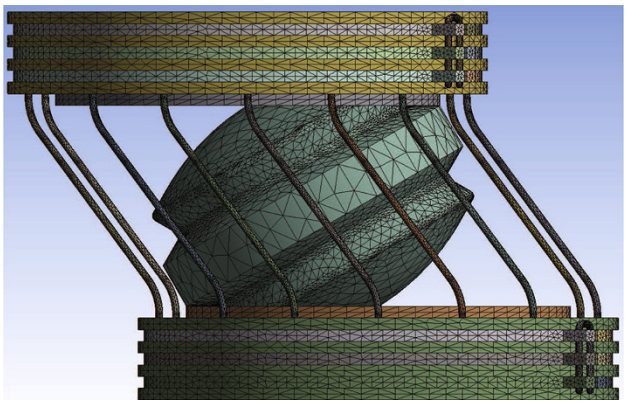

Fig. 12 Finite element meshing of the RNC isolator, to-the-left farthest deformed position

Implementation of the developed SAP2000 model into a case study

Modeling of isolated structure

Figure 18 shows a schematic diagram of the RNC-isolated linear multistory structure used in this study. The structure is symmetric 3D building of five bays, each of 8.0 m span, with double end cantilevers, each of 2.5 m length, in each horizontal direction. It has eight floors plus the isolated base floor with a typical story height of 3.0 m. The base isolated structure is modeled as a shear type supported on 36 heavy load RNC isolators, Fig. 2b, one under each column. Each floor has two lateral displacement degrees of freedom (DOF) beside one rotational DOF around the vertical axis. However, due to the symmetry of the 3D structure, only one horizontal displacement DOF is considered at each floor and is excited by a single horizontal component of earthquake ground motion in its direction. The superstructure is considered to remain elastic during the earthquake excitation and impact phenomenon. The

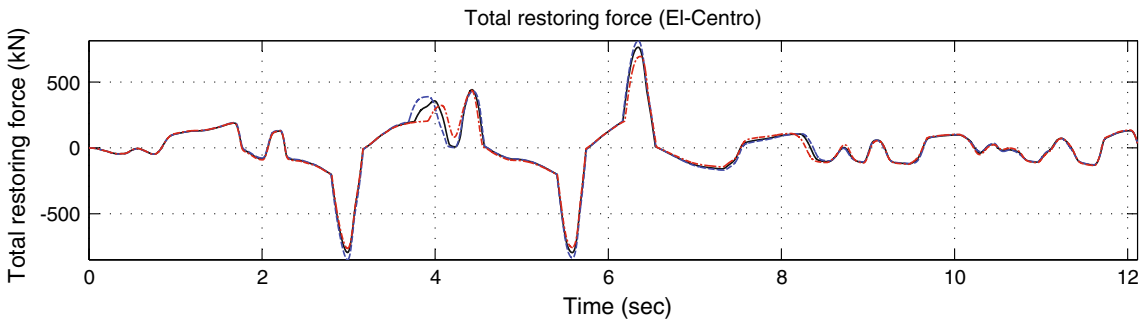

Fig. 13 Measured vs mathematical vs SAP2000 total restoring forces of the RNC isolator due to El-Centro earthquake in time scale

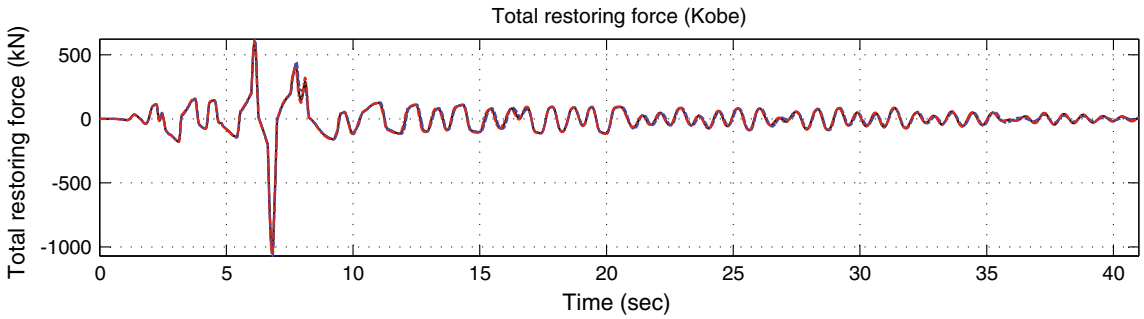

Fig. 14 Measured vs mathematical vs SAP2000 total restoring forces of the RNC isolator due to Kobe earthquake in time scale

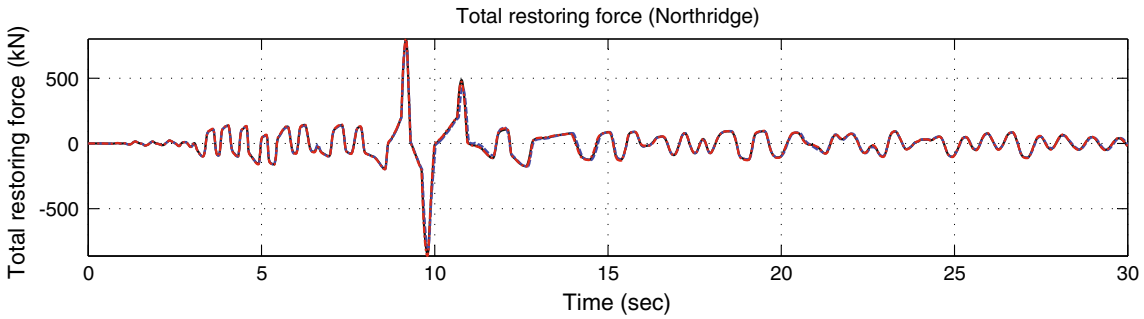

Fig. 15 Measured vs mathematical vs SAP2000 total restoring forces of the RNC isolator due to Northridge earthquake in time scale

Table 1 Numerical values of the developed SPA2000 model for the RNC isolator

SAP2000's full model parameter of RNC isolator	Value (kN, mm, s) units
Buffer stiffness	4.9033
Design displacement, Gap	300.0
Recentering stiffness	8.5808
Vertical rigidity	Infinity
Horizontal freedom	Pure roller
Hysteresis, k	3.4323
Hysteresis, yield	49.0333
Hysteresis, ratio	0.0500
Hysteresis, exp	2.5000

Table 2 Relative errors between the total measured, mathematically predicted and SAP2000 modeled restoring forces of the RNC isolator under El-Centro, Kobe and Northridge earthquakes

Models	Earthquakes					
	El-Centro		Kobe		Northridge	
	ε_1	ε_∞	ε_1	ε_∞	ε_1	ε_∞
Measured vs mathematical (%)	0.24	1.49	0.68	0.64	0.20	1.12
Measured vs SAP2000 (%)	2.95	0.62	2.52	1.67	2.57	1.97
Mathematical vs SAP2000 (%)	2.71	0.86	3.22	1.02	2.77	3.12

construction material of the isolated structure is normal weight reinforced concrete with a total material volume of 4,068.36 m^3 and the structure has a total weight of 10,170.90 tons. The structural foundation is assumed to be rigid and supported on rocky soil. The fixed-base structure has a fundamental period of 0.436 s and modal frequencies of 2.29, 6.80, 11.06, 14.94, 18.29, 21.02, 23.03 and 24.26 Hz for modes from one to eight, respectively. The structural damping ratio for all modes is fixed to 2.50 % of the critical damping.

The designed RNC isolator for this study is able to accommodate a travel design displacement, x_{des}, of 53.0 cm. Just after the selected x_{des}, the self-braking (buffer) mechanism is directly activated to stop motion over a braking distance x_{brake}. The braking distance depends mainly on pounding force intensity, F_{bB}, and the selected buffer stiffness k_b. The designed RNC isolator is 1.20 m high. The outer diameter of the upper and lower bearing steel plates is 2.0 m. It is provided with eight hysteretic mild steel dampers of the shape shown in Fig. 2b, each has a diameter of 5.0 cm. As shown in Fig. 2b, the heavy load form of the RNC isolator is provided with a linear hollow elastomeric cylinder around the rolling body to represent the main load carrying capacity, while the rolling body itself works as a secondary support in this case. The inner and outer diameters of the hollow elastomeric cylinder are

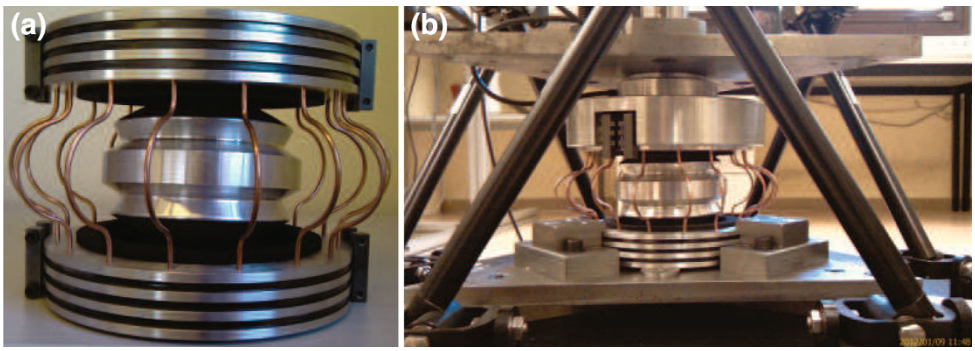

Fig. 16 Experimental small-scale prototypes of the RNC isolator before and during experimental testing (photos are published with a permission from Prof. José Rodellar, the director of CoDAlab laboratory and research group)

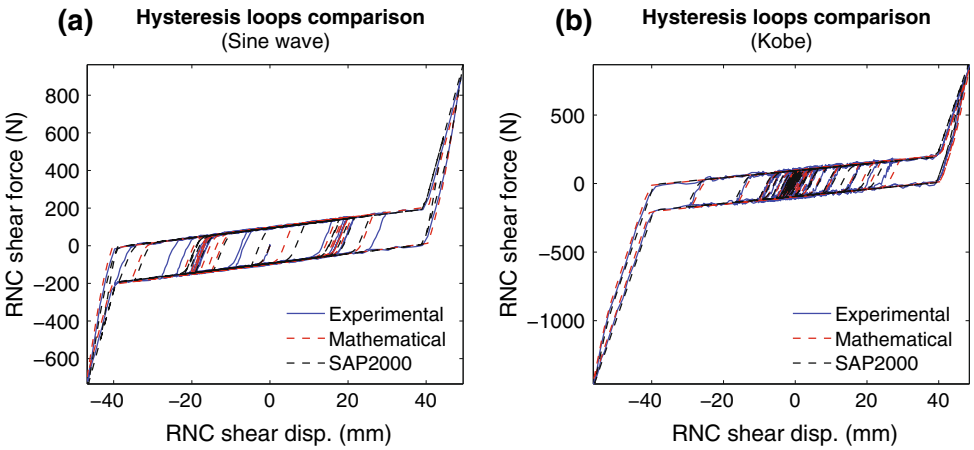

Fig. 17 Experimental, analytical and SAP2000 force displacement relationships comparison: **a** under synthetic sinusoidal excitation, **b** under reduced-amplitude real Kobe earthquake

Table 3 Relative errors between the total measured, mathematically predicted and SAP2000 modeled restoring forces of the RNC isolator under reduced-amplitudes sinusoidal and Kobe earthquakes

Models	Earthquakes			
	Sinusoidal		Kobe	
	ε_1	ε_∞	ε_1	ε_∞
Measured vs mathematical (%)	1.441	1.530	1.739	1.775
Measured vs SAP2000 (%)	2.545	1.936	2.632	1.756
Mathematical vs SAP2000 (%)	3.322	2.643	2.829	2.196

1.30 and 1.90 m, respectively. This linear elastomeric part was initially designed to follow some available recommendations of the Uniform Building Code, UBC (1997), and AASHTO, AASHTO LRFD (2005), to provide a minimum vertical load capacity of 4,000.0 kN at the extreme deformed position of buffer and to provide times that capacity at neutral non-deformed position.

Near-fault earthquakes

Near-fault (NF) ground motions are characterized by one or more intense long-period velocity and displacement pulses that can lead to a large isolator displacement (Jangid and Kelly 2001). Therefore, two sets of NF ground motions having different intensities, velocity and displacement pulses are considered to evaluate the performance of the RNC isolator's self-braking (buffer) mechanism and its influence on the structural responses. The first NF set is listed in Table 4 and comprises three pairs of ground motion components, parallel and perpendicular to the fault line, of Kobe, Northridge and San Fernando earthquakes.

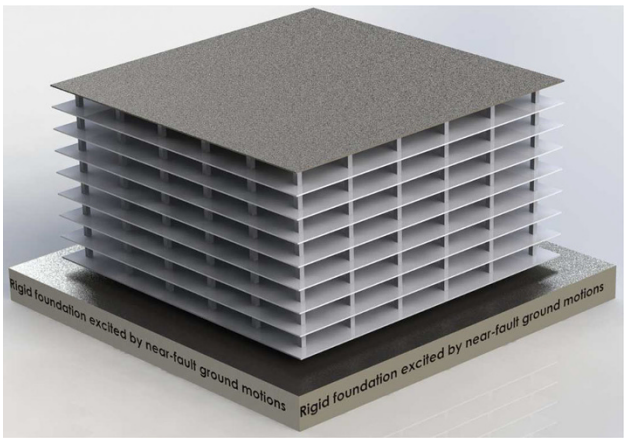

Fig. 18 Eight-story RNC-isolated structure model on a rigid foundation

Table 4 Set I of NF ground motions used in "Pounding of RNC-isolated structures with adjacent rigid structures"

No.	Earthquake name	To be applied in direction	Year	Station name	Magnitude	Peak acceleration (*g*)	
						PGA	Time
1	Kobe, Japan 0°	*X*	1995	Takarazuka	6.90	0.69	6.02
	Kobe, Japan 90°	*Y*	1995	Takarazuka	6.90	0.67	6.16
2	Northridge 18°	*X*	1994	Sylmar—conv. SE	6.69	0.83	3.51
	Northridge 288°	*Y*	1994	Sylmar—conv. SE	6.69	0.49	6.59
3	San Fernando 164°	*X*	1971	Pacoima Dam	6.61	1.23	7.76
	San Fernando 254°	*Y*	1971	Pacoima Dam	6.61	1.16	8.53

Table 5 Set II of NF ground motions used in "Inner RNC isolator's pounding and its passive mitigation"

No.	Earthquake name	Year	Station name	Magnitude	Distance to fault (km)	Peak acceleration (*g*)		Peak velocity (cm/s)		Peak displacement (cm)	
						PGA	Time	PGV	Time	PGD	Time
1	Kocaeli, Turkey 60°	1999	Yarimca	7.51	4.80	0.27	13.84	67.0	13.57	58.2	14.75
2	Imperial Valley 230°	1979	El-Centro Ar. #7	6.53	0.60	0.46	5.00	111.4	5.94	45.6	6.85
3	Kobe, Japan 0°	1995	Takarazuka	6.90	0.30	0.69	6.02	69.9	6.58	27.2	6.02
4	Northridge 18°	1994	Sylmar—conv. SE	6.69	5.20	0.83	3.51	119.8	3.44	35.1	3.02
5	San Fernando 164°	1971	Pacoima Dam	6.61	1.80	1.23	7.76	114.7	3.07	36.1	7.81

The first set's components are applied unidirectionally in *X* and *Y* directions and bidirectionally to form nine different cases of loading. Such set of NF earthquakes is used solely in "Pounding of RNC-isolated structures with adjacent rigid structures" with the aim of producing the maximum possible structural drift and structural displacement at the topmost floor of the RNC-isolated structure. The objective is to achieve severe structural pounding, with adjacent L-shaped rigid structure, before activating the RNC isolator's buffer mechanism and, then, to examine the buffer's ability to mitigate such serious structural pounding. On the other hand, the second set of NF ground motions consists of five individual components, listed in Table 5, that were selected to produce the maximum possible displacement of the RNC isolator. The individual components of that second set of NF ground motions are applied only unidirectionally to the RNC-isolated symmetric structure. The objective is to get a severe inner pounding within the RNC isolator and, then, to investigate the ability of adding more hysteresis damping to alleviate such severity of the RNC isolator's inner pounding.

Pounding of RNC-isolated structures with adjacent rigid structures

Considering the multistory structure shown in Fig. 18, this section investigates the ability of the RNC isolator's buffer mechanism to mitigate possible seismic pounding between a RNC-isolated structure with adjacent rigid structures under near-fault earthquakes considering insufficient separation gaps. Possibly, arising negative effects due to buffer activation is detected and discussed through comparing the RNC-isolated structure's responses after pounding with the corresponding response quantities of a fixed-base same structure. The adjacent structure is assumed to be of an L-shape to surround the RNC-isolated structure from two perpendicular sides, for the purpose of studying uni and bidirectional structural pounding, and to be of equal height to the RNC-isolated structure to enforce pounding at the topmost floors. Both structures are connected along their adjacent top floor perimeters by two uniaxial sets of nonlinear gap elements, available in SAP2000; one set is in the *X* direction and the other set is in *Y* direction. This enables measuring the structural pounding in both in-plan perpendicular directions under uni and bidirectional earthquake components of Table 4.

Figure 19 demonstrates the ability of the RNC isolator's buffer mechanism to eliminate, or at least to minimize, direct structural pounding under nine cases of loading. Each case of loading is named after its earthquake name followed by *X*, *Y* or *XY* characters. The *X* and *Y* notations refer to a unidirectional excitation along *X* or *Y* at a time, while the *XY* refers to a simultaneous application of bidirectional ground motion components in *X* and *Y*. In this section, the same seismic gap of 35.0 cm is considered in both *X* and *Y* directions. The designed RNC-isolated structure has an isolation period of 3.0 s. Figure 19a shows the peak pounding forces between the RNC-isolated structure and the adjacent rigid structure, in *X* and

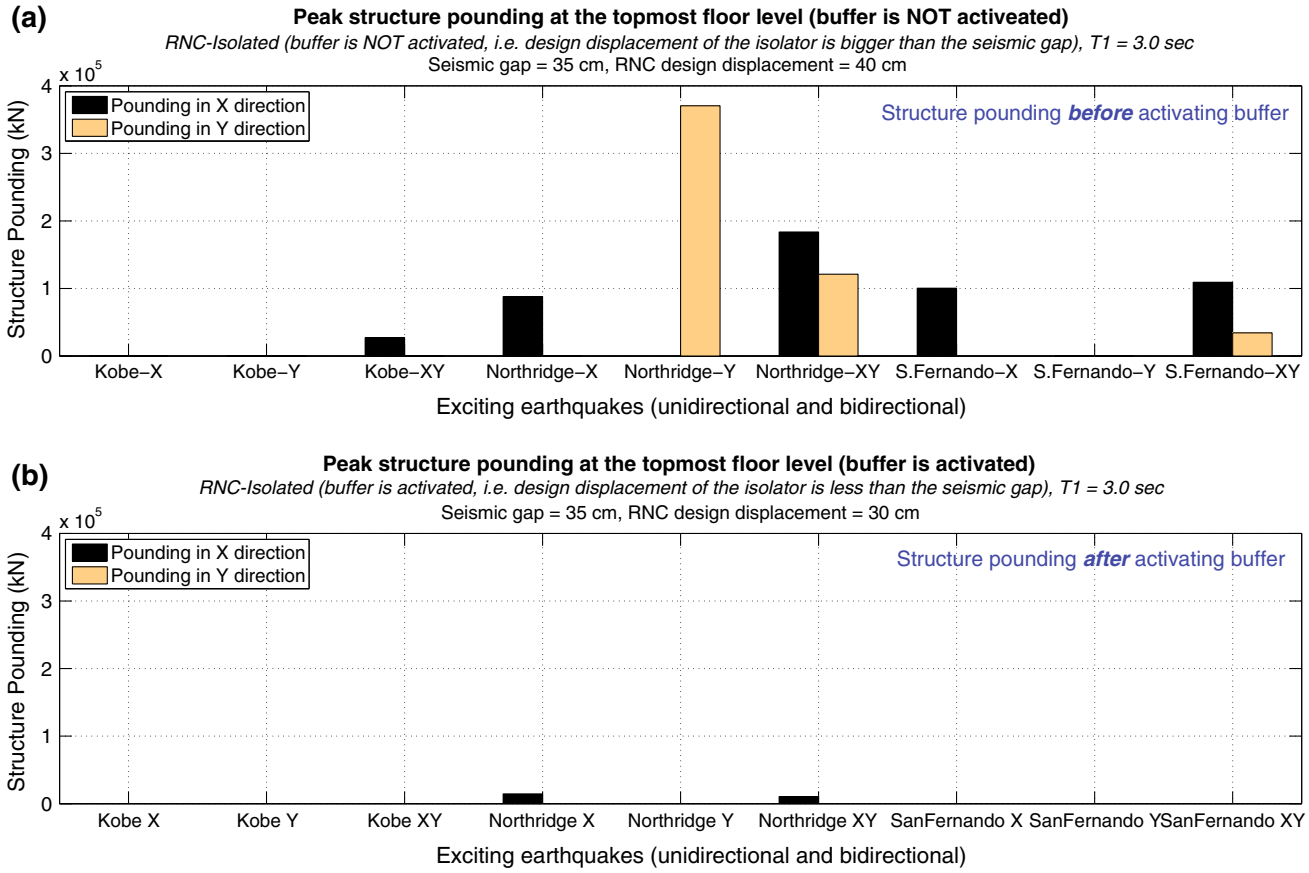

Fig. 19 Peak structure pounding with adjacent structures at the topmost floors in *X* and *Y* directions under uni and bidirectional near-fault ground motions: **a** buffer mechanism is not activated, **b** buffer mechanism is activated

Y directions, before activating the buffer mechanism of the RNC isolator. Such deactivation of the buffer mechanism is guaranteed by choosing a design displacement of the RNC isolator bigger than the actual separation seismic gap between structures. In Fig. 19a, the RNC isolator's design displacement is taken 40.0 cm to ensure buffer deactivation, while it is limited to 30.0 cm in Fig. 19b to activate the buffer mechanism before the peak bearing displacement exceeds the selected seismic gap of 35.0 cm. As a result, the influence of buffer activation on structural pounding mitigation becomes obvious through comparing both Fig. 19a and b.

Figure 19a shows that structural pounding has developed under six cases of loading with a maximum intensity of 3.70×10^5 kN in *Y* direction under the unidirectional *Y* component of the Northridge earthquake in the absence of the buffer mechanism. On the other hand, Fig. 19b shows that the buffer mechanism activation has entirely eliminated direct structural pounding under four of the six cases exhibiting pounding in Fig. 19a. The structural pounding of the remaining two cases of loading is minimized to a maximum intensity of 1.46×10^4 kN in *X* direction under the unidirectional *X* component of the Northridge earthquake. This demonstrates significant reduction of direct structural pounding under the same loading and structural conditions, besides the entire pounding elimination under two-thirds of the six cases exhibiting pounding.

The corresponding developed inner pounding within the bounds of each RNC isolator is shown in Fig. 20 under the same nine cases of loading. Figure 20a, which is corresponding to Fig. 19a, shows zero developed inner pounding inside the RNC isolator as a result of buffer deactivation. This is attributed to the selected relatively high design displacement of the RNC isolator of 40.0 cm, which must be exceeded to generate inner pounding inside the RNC isolator, what seems practically impossible under a seismic gap of 35.0 cm with a rigid structure. Contrarily, Fig. 20b, which corresponds to Fig. 19b, shows a developed inner pounding within the RNC isolator due to buffer activation. Although the peak inner RNC isolator's pounding might be comparable to the values of Fig. 19a of peak structural pounding, the activation of the RNC isolator's buffer offers more important advantages. For example, it is not only able to reduce or even cause structural pounding not to happen

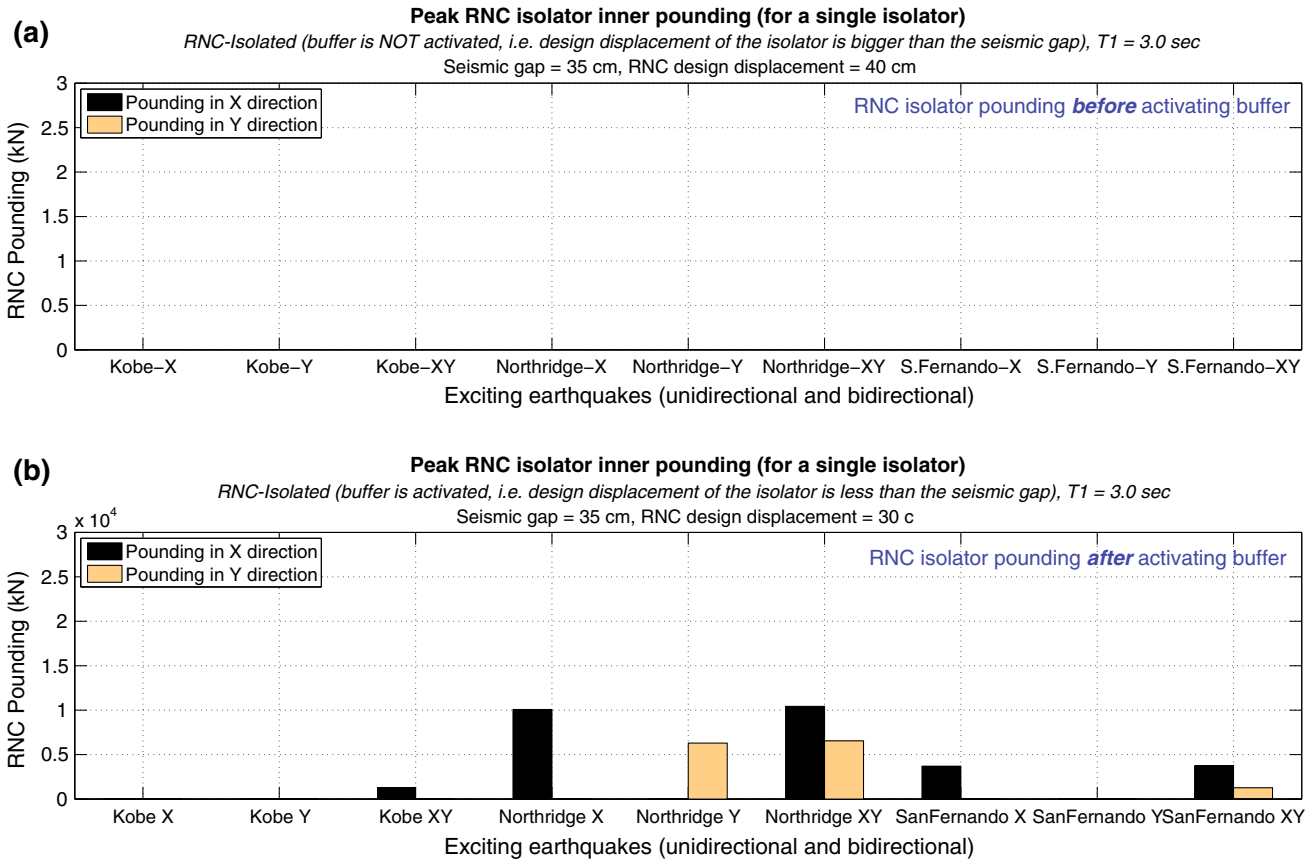

Fig. 20 Peak inner pounding of a RNC isolator in *X* and *Y* directions under uni and bidirectional near-fault ground motions: **a** buffer mechanism is not activated, **b** buffer mechanism is activated

but it also distributes pounding regularly on the isolated base floor's in-plan area and keeps pounding always within the solid metallic body of the RNC isolator. Accordingly, the RNC isolator's buffer could prevent structural pounding contact with no severe concentration of pounding forces at a local point or zone anywhere in the RNC-isolated structure, which is generally translated into less arising damage and negative effects.

The corresponding effects of RNC isolator pounding on the isolation efficiency are shown in Fig. 21 considering the peak absolute structural acceleration at the topmost floor as a performance measure. The peak absolute structural accelerations of the RNC-isolated structure, with buffer activated, is compared to those of the fixed-base same structure. Although the peak acceleration responses of the fixed-base structure are actually high, as in Fig. 21a, they could be amplified remarkably if structural or RNC isolator pounding exists. The load cases that exhibit no pounding show minimal peak structural acceleration responses. The behavior is dependent to the the interaction between the ground motion characteristics and the structural characteristics. The amplified structural accelerations due to inner RNC isolator's pounding seem to be worse (more amplified) under some loading cases and significantly reduced under some other loading cases, as shown by Fig. 21b. However, the main conclusion of this section is that the RNC isolator could powerfully mitigate or even eliminate direct structure-to-structure pounding, due to the activation of its inherent buffer mechanism, under severe NF ground motions. This could significantly reduce structural and nonstructural damage and the possibly needed repair works after strong earthquakes considering insufficient separation gaps between adjacent structures. Although, the peak structural accelerations could be amplified under some ground motions after activating the buffer mechanism. More future investigation may be required to overcome the severity of buffer pounding and, consequently, the amplification of structural acceleration responses due to buffer pounding of the RNC isolator. The next Section "Inner RNC isolator's pounding and its passive mitigation" presents a purely passive solution to alleviate the inner pounding severity and, therefore, reduce such amplification of structural acceleration responses.

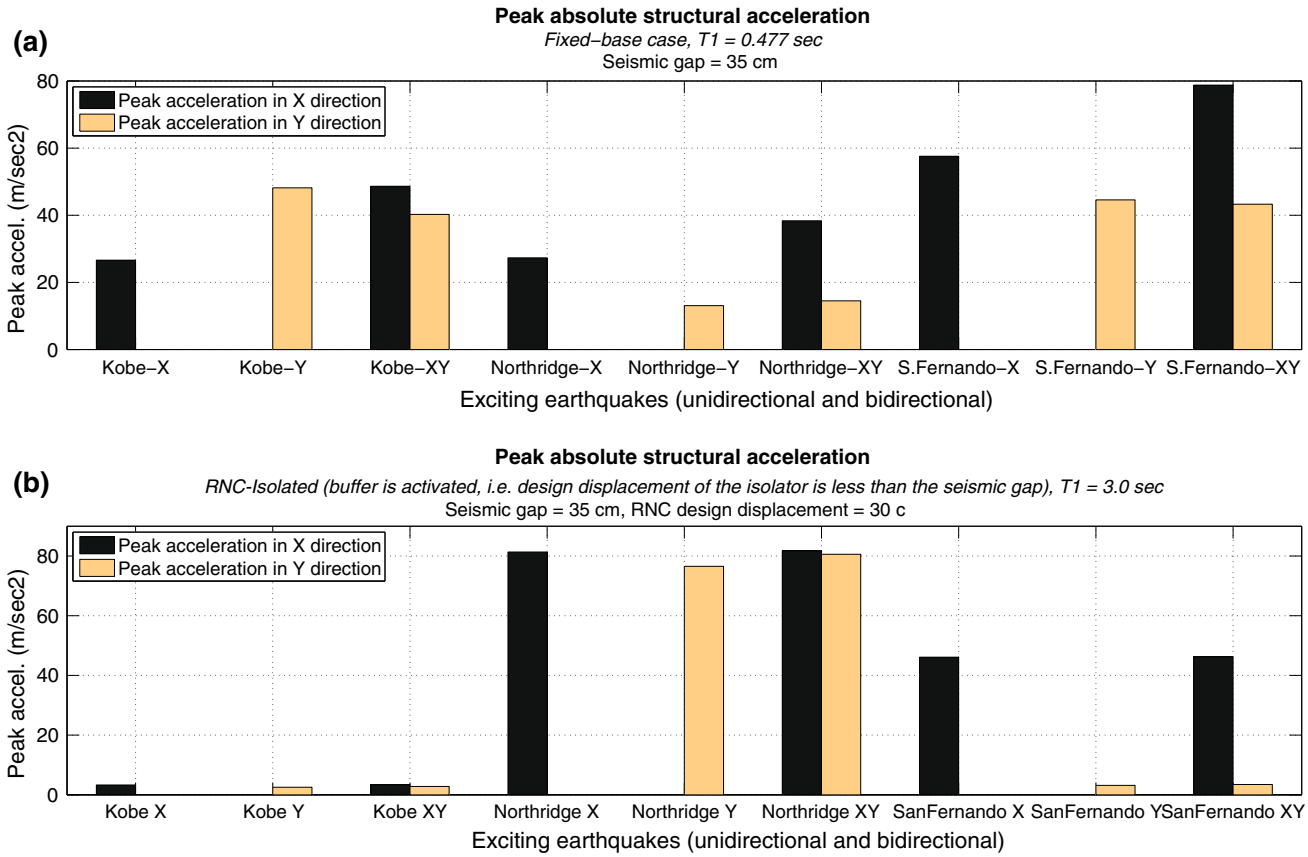

Fig. 21 Peak absolute structural acceleration in *X* and *Y* directions under uni and bidirectional near-fault ground motions: **a** fixed-base case, **b** RNC-isolated case

Inner RNC isolator's pounding and its passive mitigation

The RNC isolator is provided with a passive self-braking or buffer mechanism to maintain structural stability under severe earthquakes or to conform with limited surrounding gaps. Under such conditions, the suspended base of the RNC-isolated structure may arrive at the end of the isolator design displacement, x_{des}, when the structure still has considerable kinetic energy, due to high base velocity, causing severe inner pounding within the RNC isolator bounds. The first step to avoid or at least reduce the possible intense pounding, during preliminary design of RNC isolator, is to select a design displacement, x_{des}, that accommodates a travel distance a bit larger than that which would occur during the design earthquakes. If the selected x_{des} is not enough to alleviate pounding severity and to conform with limited surrounding gaps, another alternative is to be sought. This section investigates the ability of increasing the amount of inherent hysteretic damping, of the RNC isolator, as another possible non-expensive alternative to achieve that targets considering rigorous near-fault earthquakes.

Hysteretic damping estimation of the RNC isolator

The RNC isolator is provided with a set of triple-curvature metallic yield dampers, as shown in Figs. 1 and 2, which render the device a hysteretic behavior. Such curvatures are designed to allow for smooth extension and contraction of dampers during motion, provide adequate dampers' length for unrestrained rolling up to buffer and to reduce or avoid stress concentrations at bends to increase the dampers working life. So far, the selection of dampers number, material and dimensions to provide a specific effective damping ratio is carried out by trial and error. In this study, eight mild steel dampers are selected, each of 5.0 cm diameter. To estimate the provided effective damping of the RNC isolator used in this study, it is modeled using ADINA, a finite element analysis software (ADINA documentation 2011). Then, it is subjected to cyclic horizontal shear displacement at different shear strain amplitudes up to 100 % at loading frequency of 1 Hz. The resulting shear force–displacement relationship is plotted against the shear strain amplitudes in Fig. 22. From these hysteresis loops, the effective damping ξ of the RNC isolator was calculated using the following relationship:

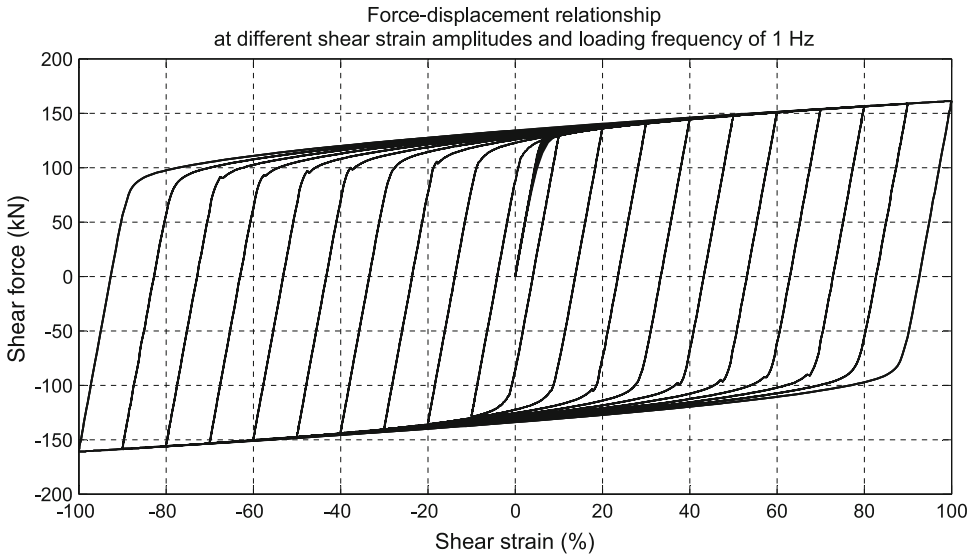

Fig. 22 The force–displacement relationship of the RNC isolator at different shear strain amplitudes

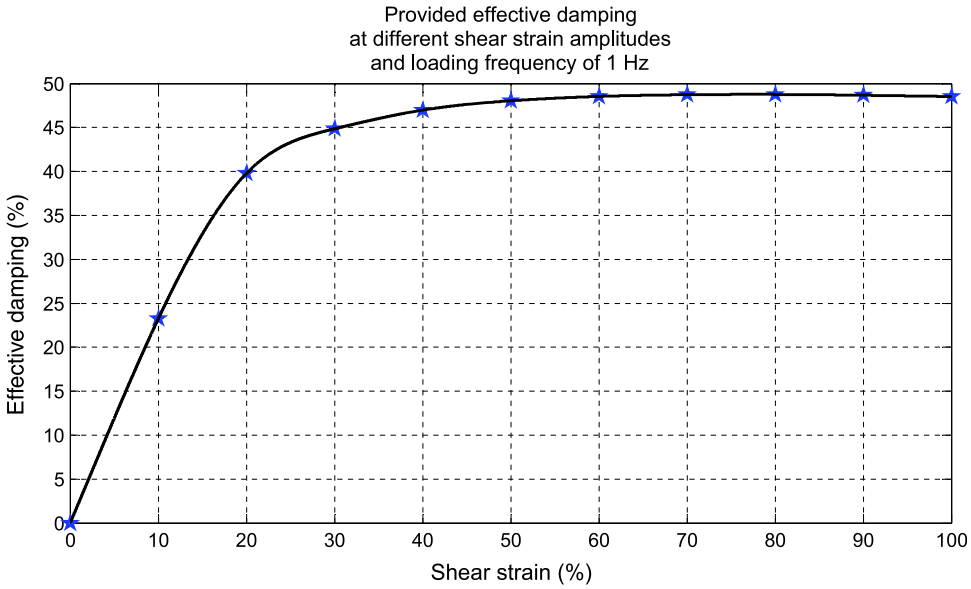

Fig. 23 RNC isolator damping vs shear strain

$$\xi = \frac{A_{\text{loop}}}{2\pi F_{\max} d_{\max}} \eta \tag{11}$$

where $F_{\max}$ is the peak value of the shear force, $d_{\max}$ is the peak value of the shear displacement, A_{loop} is the hysteresis loop area, η is the number of metallic yield dampers.

The damping ratio is plotted as a function of the shear strain in Fig. 23, where the damping ratio goes up rapidly to a relatively high value of 48.76 % then remains almost constant as the shear strain increases. The ability of this high damping ratio, provided by the low-cost metallic yield dampers, to limit the bearing displacement and pounding severity is investigated herein under the NF earthquakes of "Near-fault earthquakes".

Influence of hysteretic damping on possible pounding severity

Three structures are employed in the parametric study of this section: the one described in "Modeling of isolated structure" the same structure but once is 25 % lighter in weight and the other time is 25 % heavier. This to investigate the influence of the isolated structural weight on bearing displacement and pounding intensity. On the other hand, to investigate the influence of the provided amount of hysteretic damping by the RNC isolator on the bearing displacement and consequently on pounding, three additional designs of the RNC isolator, of the form mentioned in "Modeling of isolated structure", are considered. They

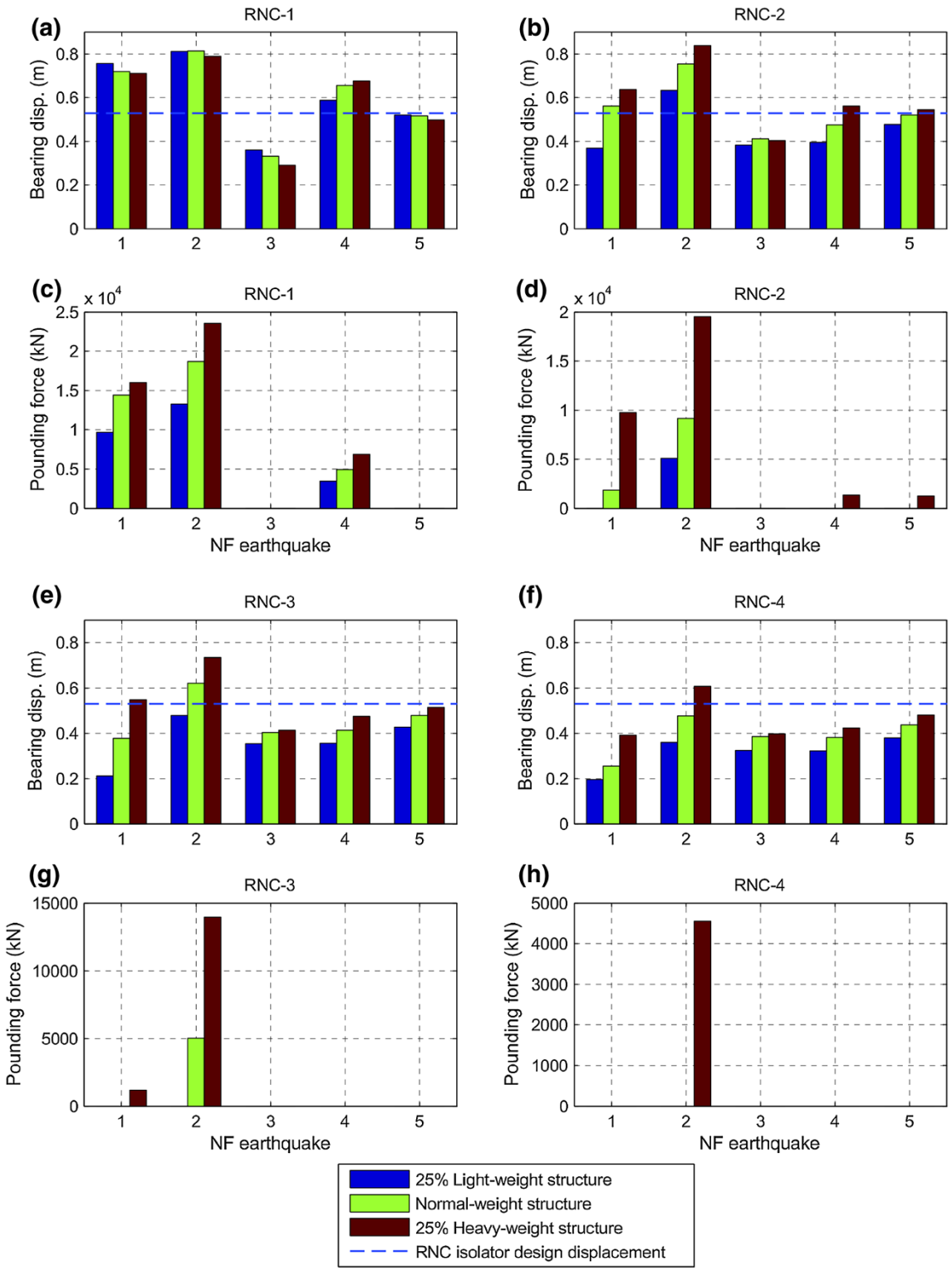

Fig. 24 Effect of structural weight and hysteretic damping on bearing displacement and pounding intensity: **a** bearing displacement using RNC-1 isolator, **b** bearing displacement using RNC-2 isolator, **c** pounding force using RNC-1 isolator, **d** pounding force using RNC-2 isolator, **e** bearing displacement using RNC-3 isolator, **f** bearing displacement using RNC-4 isolator, **g** pounding force using RNC-3 isolator, **h** pounding force using RNC-4 isolator

Table 6 Peak absolute structural accelerations using different RNC isolators with and without buffer mechanisms, m/s^2 units

Earthquake number	Fixed base	RNC-1				RNC-2				RNC-3				RNC-4			
		No buffer	%	With buffer	%	No buffer	%	With buffer	%	No buffer	%	With buffer	%	No buffer	%	With buffer	%
25 % lighter structure																	
1	7.35	0.890	88	15.883	−116	1.095	85	1.095	85	1.487	80	1.487	80	1.946	74	1.946	74
2	9.50	1.129	88	22.698	−139	1.534	84	11.442	−20	1.790	81	1.790	81	2.351	75	2.351	75
3	19.91	1.028	95	1.028	95	1.684	92	1.684	92	1.912	90	1.912	90	2.334	88	2.334	88
4	28.77	0.711	98	5.028	83	1.282	96	1.282	96	1.590	94	1.590	94	2.078	93	2.078	93
5	53.01	1.092	98	1.092	98	1.693	97	1.693	97	1.808	97	1.808	97	2.246	96	2.246	96
Normal weight structure																	
1	11.35	0.616	95	14.538	−28	0.988	91	4.209	63	1.176	90	1.176	90	1.508	87	1.508	87
2	15.15	0.924	94	22.809	−51	1.329	91	16.814	−11	1.495	90	8.783	42	1.745	88	1.745	88
3	24.66	1.064	96	1.064	96	1.498	94	1.498	94	1.521	94	1.521	94	1.741	93	1.741	93
4	21.55	0.654	97	9.104	58	0.996	95	0.996	95	1.285	94	1.285	94	1.664	92	1.664	92
5	44.26	0.728	98	0.728	98	1.265	97	1.265	97	1.530	97	1.530	97	2.000	95	2.000	95
25 % heavier structure																	
1	10.51	0.486	95	14.652	−39	0.847	92	10.994	−5	1.057	90	3.067	71	1.287	88	1.287	88
2	13.32	0.746	94	22.773	−71	1.206	91	19.280	−45	1.355	90	12.683	5	1.525	89	7.324	45
3	27.89	0.696	98	0.696	98	1.207	96	1.207	96	1.288	95	1.288	95	1.525	95	1.525	95
4	19.56	0.566	97	10.414	47	0.958	95	1.769	91	1.104	94	1.104	94	1.375	93	1.375	93
5	34.22	0.680	98	0.680	98	1.154	97	3.445	90	1.230	96	1.230	96	1.639	95	1.639	95

provide 75, 50 and 25 % less damping than the above main designed RNC isolator, and referred to as RNC-1, RNC-2, RNC-3, respectively, while the main RNC isolator design of highest damping is denoted with RNC-4, i.e., the higher the number the higher the provided damping. Then, all the RNC-isolated structures are subjected to the five earthquakes of "Near-fault earthquakes", one at a time, and the resulting bearing displacements as well as the pounding forces are displayed in Fig. 24. Each earthquake is referred to by its serial number found in the first column from left of Table 5. All the response quantities in this section are obtained by simulating the RNC-isolated structures using SAP2000. The RNC isolator is represented in SAP2000 using its developed model in "SAP2000 modeling of the RNC isolator". The structure floors were modeled as rigid horizontal diaphragms while the columns are modeled with zero axial deformation and the structural mass is lumped at floor levels.

The bearing displacements of RNC isolators RNC-1, RNC-2, RNC-3 and RNC-4 are displayed in Fig. 24a, b, e and f, respectively. The corresponding pounding forces are shown in Fig. 24c, d, g and h, respectively, considering different structural weights and NF excitations. It seems evident that increasing the isolator hysteretic damping produces a decrease in the bearing displacement and consequently eliminates or at least alleviates the pounding intensity, although the heavier isolated structures are less responsive to increasing the isolators damping. Figure 24 also demonstrates that pounding is always more intense in the case of isolated heavy structures, even if they exhibit closer bearing displacements to those of isolated lighter structures. Moreover, the pounding intensity is directly proportional to the amount of extra base displacement beyond the bearing design displacement x_{des}.

Near-fault ground motions are rich in long-period frequencies. This can lead to resonance conditions with seismically isolated structures of long fundamental periods causing undesirable higher bearing displacements. Such resonance seems obvious in this study under the first two earthquakes, particularly, using RNC-1 and RNC-2 isolators. Although the Kocaeli and the Imperial Valley earthquakes have the lowest PGA in Table 5, the resulting bearing displacements are the highest, even are higher than those produced by San Fernando earthquake, which has the highest PGA among the used earthquakes. This is mainly attributed to the close structural and loading, dominant, frequencies.

Based on the above results, adding more hysteretic damping to the RNC isolator improves the behavior of the isolated structures in terms of reducing the bearing displacements and the resulting pounding intensity, if there is any. But, practically, this solution should not obstruct the

isolator itself to achieve efficient isolation regarding reducing the peak absolute structural accelerations. To investigate that, the corresponding peak absolute structural accelerations of the case study shown in Fig. are obtained and listed in Table 6. The performance measure is taken as the reduction percentage of acceleration responses. This percentage (%) is expressed as:

$$\% = \frac{(\ddot{x}_{\text{fixed-base}}) - (\ddot{x}_{\text{RNC-isolated}})}{(\ddot{x}_{\text{fixed-base}})} \times 100 \quad (12)$$

where $\ddot{x}_{\text{fixed-base}}$ is the peak acceleration of fixed-base structure and $\ddot{x}_{\text{RNC-isolated}}$ is the peak acceleration of RNC-isolated structure. The negative values of % in Table 6 indicates the undesired negative effect of pounding on structural accelerations. From this table, the following conclusions could be drawn:

1. Increasing the isolator hysteretic damping slightly reduces the peak accelerations of the isolated structure.
2. At low provided damping levels, intense pounding of an isolated structure results in structural accelerations higher than those of its fixed-base case. This becomes more obvious in structures with relatively light weight. However, adding more non-expensive inherent damping can significantly improve that terrible conditions.
3. Increasing the isolator hysteretic damping can remarkably attenuate the undesirable increase of the structural accelerations due to pounding.
4. The RNC isolator can achieve high levels of structural accelerations reduction, especially under severe ground motions.
5. Where there is no pounding, isolation of light weight structures is less efficient under low-intensity earthquakes compared to heavier structures under the same earthquakes. This isolation efficiency becomes higher under more severe earthquakes showing similar behavior to that of heavier structures under such strong earthquakes.

Conclusions

This paper presents a full-feature representation of the Roll-N-Cage (RNC) isolator using a commercially available finite element code, referred to as SAP2000, to provide a powerful and handy model of the device using a popular software in the area of structural engineering. The developed SAP2000 model considers all the main and unique features of the RNC isolator including self-recentering, hysteretic damping, self-braking (buffer), design displacement, vertical rigidity, horizontal flexibility, no uplift, post- and pre-yield stiffness. The obtained model is then validated numerically, analytically and experimentally. The discrepancy between the three representations of the RNC isolator quantified using L_1 and L_∞-norms with effectively small errors. The obtained validated SAP2000 model is then implemented into a real problem of mitigating direct pounding of a RNC-isolated structure with a adjacent structures, considering insufficient separation gaps in near-fault zones, by means of the RNC isolator's buffer mechanism. Finally, the paper has addressed the problem of passive mitigation of the possible inner pounding that may arise within the RNC isolator under severe near-fault earthquakes. Three main conclusions are found. Firstly, the developed SAP2000 model for the RNC isolator could be a precise and powerful replacement of the device in more future professional and research studies. Secondly, the inherent buffer mechanism of the RNC isolator could successfully reduce or even prevent direct structure-to-structure pounding under severe near-fault ground motions. Thirdly, increasing the amount of provided non-expensive hysteretic damping of the RNC isolator could efficiently reduce the bearing displacement to be within affordable design limits and, consequently, eliminates or at least reduces pounding intensity to remarkable extents and, therefore, reduces possible structural response amplification due to buffer activation.

Acknowledgments The first author gratefully acknowledges the financial support of professor José Rodellar, the director of CoDAlab laboratory and research group at the Technical University of Catalonia in Spain, to entirely accomplish the experimental validation of the RNC isolator.

References

AASHTO LRFD (2005) Bridge design specifications, SI units, 3rd edn. American Association of State Highway and Transportation Officials

ADINA Documentation (2011) Release 8.73. ADINA R & D Inc, Watertown

Al-Hussaini T, Zayas V, Constantinou M (1994) Seismic isolation of a multi-story frame structure using spherical sliding isolation systems. In: Technical report, NCEER-94-0007. National Center of Earthquake Engineering Research, Buffalo

Constantinou M, Adnane M (1987) Dynamics of soil-base-isolated structure systems: evaluation of two models for yielding systems. In: Report to NSAF, Department of Civil Engineering, Drexel University, Philadelphia

Constantinou M, Symans M (1993) Seismic response of structures with supplemental damping. Struct Des Tall Build 2(2):77–92

Derham C, Kelly J, Tomas A (1985) Nonlinear natural rubber bearings for seismic isolation. Nucl Eng Des 84(3):417–428

Grigoriev I, Meilikhov E, Radzig A (1996) Handbook of physical quantities. CRC Press, Boston

Ikhouane F, Rodellar J (2005) On the hysteretic Bouc–Wen model. Part I: forced limit cycle characterization. Nonlinear Dyn 42:63–78

Ikhouane F, Mañosa V, Rodellar J (2007) Dynamic properties of the hysteretic Bouc–Wen model. Syst Control Lett 56:197–205

Ismail M (2009) An innovative isolation device for aseismic design. PhD Thesis, Doctoral program, Earthquake engineering and structural dynamics, vol 20, p 08, Technical University of Catalonia, Barcelona. http://www.tdx.cat/handle/10803/6265. Accessed 10 October 2009

Ismail M, Rodellar J (2014a) Experimental mechanical characterization of a rolling-based seismic isolation system. In: 6th World conference on structural control and monitoring, Barcelona, 15–17 July 2014

Ismail M, Rodellar J (2014b) A multi-purpose testing platform using hexapod. In: 6th World conference on structural control and monitoring, Barcelona, 15–17 July 2014

Ismail M, Rodellar J, Ikhouane F (2008) A seismic isolation system for supported objects. Spanish patent no. P200802043, Spanish Office of Patents and Marks

Ismail M, Ikhouane F, Rodellar J (2009a) The hysteresis Bouc–Wen model, a survey. J Arch Comput Methods Eng 16:161–188

Ismail M, Rodellar J, Ikhouane F (2009b) Performance of structure-equipment systems with a novel roll-*n*-cage isolation bearing. Comput Struct 87:1631–1646

Ismail M, Rodellar J, Ikhouane F (2010) An innovative isolation device for aseismic design. J Eng Struct 32:1168–1183

Ismail M, Casas J, Rodellar J (2013) Near-fault isolation of cable-stayed bridges using RNC isolator. Eng Struct 56:327–342

Jangid R, Kelly J (2001) Base isolation for near-fault motions. Earthq Eng Struct Dyn 30:691–707

Jurukovski D, Rakicevic Z (1995) Vibration base isolation development and application. In: Duma (ed) 10th European conference on earthquake engineering, Balkema, pp 667–676

Kelly J (1986) Seismic base isolation: review and bibliography. Soil Dyn Earthq Eng 5:202–216

Ma F, Zhang H, Bockstedte A, Foliente G, Paevere P (2004) Parameter analysis of the differential model of hysteresis. J Appl Mech ASME 71:342–349

Murnal P, Sinha R (2004) Aseismic design of structure–equipment systems using variable frequency pendulum isolator. Nucl Eng Des 231:129–139

Naeim F, Kelly J (1999) Design of seismic isolated structures—from theory to practice. Wiley, New York

Robinson W, Tucker A (1977) A lead-rubber shear damper. Bull N Z Natl Soc Earthq Engl Natl Soc Earthq Eng 10(3):151–153

Robinson W, Tucker A (1983) Test results for lead-rubber bearings for the William M. Clayton building, Toe Toe bridge, and Waiotukupuna bridge. Bull N Z Natl Soc Eng 14(1):21–33

SAP2000 Documentation (2012) Release 15.1.0. Computer and Structure Inc, Berkeley

Skinner R, Robinson W, McVerry G (1993) An introduction to seismic isolation. Wiley, Chichester

Staudacher K (1982) Integral earthquake protection of structures IV: full base isolation and seismic mass analogy. In: Technical report, Eidgenossische Technische Hochschule (Zurich), Inst. für Baustatikund Konstruktion, Bericht 134, Birkhauser Verlag, Basel

Tyler R, Robinson W (1984) High-strain tests on lead-rubber bearings for earthquake loadings. Bull N Z Natl Soc Earthq Eng 17:90–105

(1997) Uniform building code. In: International conference of building officials, California

Wen Y (1976) Method for random vibration of hysteretic systems. J Eng Mech Div 102(EM2):246–263